

DISSERTATION ON  
**DYE SENSITIZED SOLAR CELLS**

PROJECT REPORT SUBMITTED TO THE  
DEPARTMENT OF PHYSICS  
INTEGRAL UNIVERSITY, LUCKNOW



IN PARTIAL FULFILMENT FOR THE DEGREE OF  
**MASTER OF SCIENCE**  
**IN PHYSICS**

**SUBMITTED BY**  
**NAUMAN RAZA**  
**ENROLLMENT NO: 2000102441**

UNDER THE SUPERVISION OF  
**DR. SYED SALMAN AHMAD WARSI**  
DEPARTMENT OF PHYSICS  
**INTEGRAL UNIVERSITY LUCKNOW, 226026**

**2022**



# INTEGRAL UNIVERSITY

Established Under the Integral University Act 2004(U.P. Act No.9 of 2004)

Approved by University Grant Commission under Sessions 2(f) and 12B

Phone No: +91(0522)2890812, 2890730, 6451039, Fax No: 0522-2890809

Kursi Road, Lucknow-226026, Uttar Pradesh (INDIA)

## CERTIFICATE FROM SUPERVISOR

---

This is to certify that the PG Physics Project (PY508) on ' **DYE SENSITIZED SOLAR CELLS** submitted by **NAUMAN RAZA** the candidate with enrollment number (2000102441), in partial fulfilment of requirements for the award of the degree of M.Sc.(Physics) at the department of Physics, Integral University, Lucknow, is a record of the candidate's work studied by him under the supervision of **DR. SYED SALMAN AHMAD WARSI**. The dissertation was a compulsory part of his M.Sc. (Physics) degree.

**DR. SYED SALMAN AHMAD WARSI**

(SUPERVISOR)

INTEGRAL UNIVERSITY



Established Under the Integral University Act 2004(U.P. Act No.9 of 2004)

Approved by University Grant Commission under Sessions 2(f) and 12B

Phone No: +91(0522)2890812, 2890730, 6451039, Fax No: 0522-2890809

Kursi Road, Lucknow-226026, Uttar Pradesh (INDIA)

### CERTIFICATE BY HEAD OF DEPARTMENT

---

This is to certify that the PG Physics Project (PY508) on 'Study of the **DYE SENSITIZED SOLAR CELLS** submitted by the candidate **Nauman Raza** with enrollment number (2000102441), award of the degree of in partial fulfilment of requirements for the M.Sc.(Physics) at the department of Physics, Integral University, Lucknow, is a record of the candidate's work studied by him under the supervision of Dr Syed Salman Ahmad Warsi . The dissertation was a compulsory part of his M.Sc.(Physics) degree.

Date:

(Dr. Seema Srivastava)

Head, Department of Physics

Integral University

## **DECLARATION**

I here declare the project work entitled '**DYE SENSITIZED SOLAR CELLS**' submitted to the Integral University Lucknow , in partial fulfilment of the requirement for the degree of Master of Science (Physics) is the result of original work carried out by me under the supervision of Dr.Syed Ahmad Warsi

Nauman Raza

Enrollment no. 2000102441

## **ACKNOWLEDGEMENT**

I would like to express my special thanks of gratitude to my supervisor Dr. Syed Salman Ahmad Warsi for providing me this golden opportunity to present my project under his supervision. Throughout the project he provided me constant support, invaluable guidance and motivation.

My thankfulness also goes to Dr. Seema Srivastava , Head of Department of Physics, and Integral University for making sure the necessary facilities in this project.

Finally, I would like to express my deepest gratitude to GOD and my family for making me what I am today. I also want to thank my all friends for their help.

I am eternally grateful to everyone for their love and blessings.

**NAUMAN RAZA**

# CONTENT

|                                   |              |
|-----------------------------------|--------------|
| Certificate of Supervisor         | i            |
| Certificate of Head of Department | ii           |
| Declaration                       | iii          |
| Acknowledgement                   | iv           |
| Contents                          | v            |
| List of Abbreviation              | vi           |
| List of Figures & Tables          | vii          |
| <b>CHAPTER 1</b>                  | <b>1-18</b>  |
| <b>1. INTRODUCTION</b>            |              |
| 1.1 Solar Cell                    |              |
| 1.2 DSSCS                         |              |
| 1.3 Counter Electrode             |              |
| <b>CHAPTER 2</b>                  | <b>19-24</b> |
| <b>2. ELECTROLYTE</b>             |              |
| 2.1 Liquid Electrolyte            |              |
| 2.2 Solid Electrolyte             |              |
| 2.3 Quasi Solid State Electrolyte |              |
| <b>CHAPTER 3</b>                  | <b>25-37</b> |
| <b>3. DYES</b>                    |              |
| 3.1 Development in Dye Synthesis  |              |

3.2 N3/N719/N712 Dyes

3.3 Metal Free Organic Dyes

3.4 Coumarin Dyes

3.5 Indole Dyes

3.6 Triarylamine Dyes

3.7 Phenothiazine Dyes

3.8 Carbazola Dyes

3.9 Natural Dyes

|                                     |              |
|-------------------------------------|--------------|
| <b>LATEST APPROACHES AND TRENDS</b> | <b>37-39</b> |
| <b>CONCLUSION</b>                   | <b>40-41</b> |
| <b>REFERENCES</b>                   | <b>42-53</b> |

## LIST OF ABBREVIATIONS

ACN: Acetonitrile;  
Ag NPs: Silver nanoparticles;  
AM : Air mass;  
BODIPY: Boradiazaindacene  
; BPI: 4,5-Bis(4- methoxyphenyl-1H-imidazole) ; Carbon;  
CBZ: Carbazole  
CDCA: Chenodeoxycholic acid;  
CdSe: Cadmium selenide;  
CNE: Carbon nanofiber;  
CNI: Carbon nanotube;  
CPEs: Conjugated polymer electrolytes;  
CuBr: Copper bromide;  
CuI: Copper iodide;  
CuSCN: Copper thiocyanate;  
CV: Cyclic voltammetry;  
DPP: Diketopyrrolopyrrole;  
DSSCDB: Dye-sensitized solar cell database;  
DSSCs: Dye-sensitized solar cells;  
EC: Ethylene carbonate;  
EIS: Electron impedance spectroscopy;  
EPFL: Ecole Polytechnique Fédérale de Lausanne;  
ERDs: Energy relay dyes;  
FF: Fill factor;  
FRET: Fluorescence (Forster) resonance energy transfer;  
FTO: Fluorine-doped tin oxide;  
GA: Glucuronic acid;  
GBL:  $\gamma$ -Butyrolactone;  
GusCN: Guanidinium thiocyanate;  
HfO<sub>2</sub>: Hafnium

## **List of figures**

1. Figure : 1 Photo electric effect of PV cell
2. Figure : 2 The performance of dye PV modules increases with temperature, contrary to Si-based modules
3. Figure : 3 Construction and working principle of the dye-sensitized nanocrystalline solar cells
4. Figure : 4 I-Vcurve to evaluate the cells performance
5. Figure : 5 Optical transmittance of platinum-based films deposite onto FTO glass
6. Figure : 6 The a current density-voltage -) and b incident monochromatic photon-to-current conversion efficiency (PCE) Curves of DSSCs using various  $\text{Cu}_2\text{O}$  CE
7. Figure : 7 Nyquist plots of the Device\_FTO and Device\_Mo
8. Figure : 8 Raman spectra of mangosteen peel carbon
9. Figure : 9 Polarization curves of DSSCs
10. Figure : 10 UV-vis spectroscopy selected pyridinium and imidazolium salts.
11. Figure : 11 Molecular structure of Ruthenium complex based dye sensitizers
12. Figure : 1 2 Molecular Structure of metal-free organic dyes
13. Figure : 13 Molecular structure of Coumarin and indole
14. Figure : 14 HOMO and LUMO energy level diagram of dyes IK 3-6
15. Figure : 15 Chemical structures of anthocyanin, flavonoid, beta beta-carotene, and d chlorophyll
16. Figure : 16 IPCE of mixed pigment and single pigments,
17. Figure: 17 a Nyquist plots obtained from the EIS of DSSCs with varying  $\text{Ag}@\text{SiO}_2$  content (inset shows the equivalent circuit). b  $R_2$  ohm with respect to the  $\text{Ag}@\text{SiO}_2$  NPs content

## **LIST OF TABLE**

1. Photovoltaic parameters of DSSCs employing differenttypes of WEs and CE
2. Efficiencies for different dyes and electrolytes
3. Absorption spectra and photoelectric performance for DSSCS based on different metal complex [polypyridyl (Ru)] dye
4. The efficiency for DSSCs based on different metal-free organic dyes
5. Availability and color range for the natural dyes (anthocyanin, carotenoid, chlorophyll, and flavonoid)

# 1.CHAPTER

## INTRODUCTION

### **SOLAR CELL**

A solar cell or photovoltaic cell which is based on the photoelectric effect, is an electrical device that converts light energy directly into electricity. When a solar cell is exposed to light, its electrical properties such as voltage, resistance, current etc. changes significantly. Solar cells are the basic functional devices which constitute the solar panels. The voltage produced by a typical single junction silicon solar cell in an open circuit is typically from 0.5 volts to 0.6 volts.

Irrespective of the light source used for illumination i.e. whether it is natural or artificial, the solar cells are classified as photovoltaic. Apart from producing energy, the photovoltaic cells are also used as a photo detector near the visible range of EM radiation.

A solar cell must have three basic characteristics in order to function:

- 1 Generation of hole – electron pair (also known as excitons) by absorbing the light.
- 2 Separation of hole – electron pair.
- 3 Extraction of hole – electron pair in an external circuit

### **CONSTRUCTION OF SOLAR CELL**

A solar cell is basically a junction diode ; however it is constructed differently from traditional p-n junction diodes. On a thicker n-type semiconductor, a very thin layer of p-type semiconductor is formed. On top of the p-type semiconductor layer, we place a few finer electrodes .

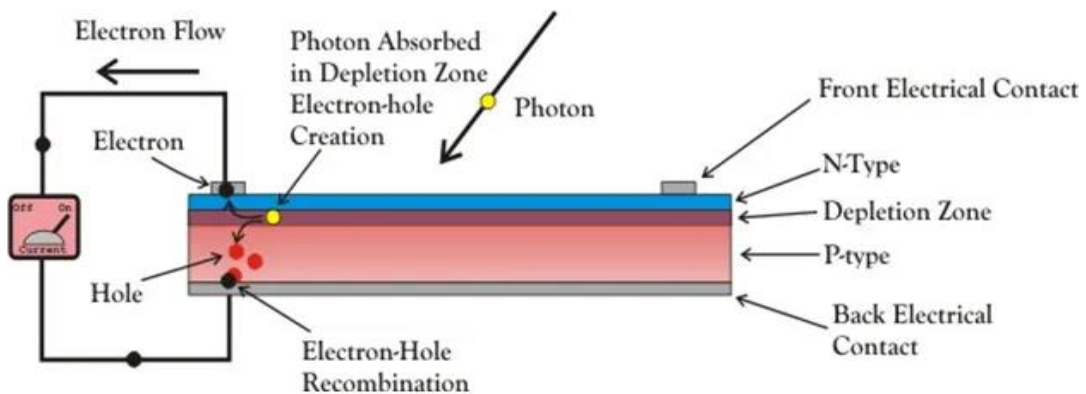


**Fig 1 Photo electric effect of PV cell**

The thin p-type layer is not obstructed by these electrodes. A p-n junction exists just under the p-type layer. A current collecting electrode is also provided at the bottom of the n-type layer. To protect the solar cell from mechanical shock, we encase the complete unit in thin glass. The thin p-type layer is not obstructed by these electrodes. A p-n junction exists just under the p-type layer. A current collecting electrode is also provided at the bottom of the n-type layer. To protect the solar cell from mechanical shock, we encase the complete unit in thin glass.

## **WORKING PRINCIPLE OF SOLAR CELL**

When light reaches the p-n junction, photons can readily pass through the thin p-type layer and into the junction. The photons in the light energy supply the junction with enough energy to build a number of electron-hole pairs. The incident light breaks the thermal equilibrium condition of the junction. The depletion region's free electrons can quickly reach the n-type side of the junction.

Similarly, depletion holes can quickly reach the p-type side of the junction. The newly created free electrons cannot cross the junction once they reach the n-type side due to the junction's barrier potential.

Similarly, as the newly created holes reach the p-type side of the junction, they become of the same barrier potential as the junction. The p-n junction will behave like a tiny battery cell when the concentration of electrons increases on one side, i.e. the n-type side of the junction, and the concentration of holes increases on the other side, i.e. the p-type side of the junction. A photo voltage is produced. A modest current will flow through the junction if we attach a small load across it.

## **MATERIALS USED IN SOLAR CELL**

The materials which are used for this purpose must have band gap close to 1.5eV. Commonly used materials are-

- Si Silicon.
- Gallium arsenide (GaAs)
- Cadmium telluride (CdTe)
- Copper Indium Selenium (CuInSe<sub>2</sub>)

## Criteria for Materials to be Used in Solar Cell

- Must have band gap from 1ev to 1.8ev.
- It must have high optical absorption.
- It must have high electrical conductivity.
- The raw material must be available in abundance and the cost of the material must be low.

### ➤ **ADVANTAGES OF SOLAR CELL**

- No pollution associated with it.
- It must last for a long time.
- No maintenance cost.

### ➤ **DISADVANTAGES OF SOLAR CELL**

- It has high cost of installation.
- It has low efficiency.
- The energy cannot be produced on cloudy days, and we will not receive solar energy at night.

### ➤ **USES OF SOLAR GENERATION SYSTEMS**

- It may be used to charge batteries.
- Used in light meters.
- It is used to power calculators and wrist watches.
- It can be used in spacecraft to provide electrical energy.

## **WHAT IS DSSCS**

Dye-sensitized solar cells (DSSCs) absorb incoming sunlight with an organic dye, which produces excited electrons and energy, which is then transferred to a cheap substance like titanium dioxide (TiO<sub>2</sub>). The energy is gathered on a transparent conducting surface after that. Carmine, santalin are two natural dyes, were chosen as potential sensitizers for dye-sensitized solar cells. Natural dyes' power conversion efficiency was about 0.5 percent compared to LEG4's (5.6 percent) under identical conditions, owing to lower open circuit potentials and photocurrent densities.

### ➤ **ADVANTAGES**

- Cost effectiveness ease of manufacture,
- simple manipulation

➤ **ADVANTAGES OF ADOPTING DSSCS.**

They perform better under greater temperature circumstances and diffused light than conventional solar cells. The efficiency of DSSC conversion for various dyes and metal oxides.

➤ **DISADVANTAGES**

The major disadvantage to the DSSC design is the use of the liquid electrolyte, which has temperature stability problems. At low temperatures the electrolyte can freeze, halting power production and potentially leading to physical damage.

DSSCs (dye-sensitized solar cells) have emerged as a technically and economically viable alternative to p-n junction photovoltaic. It was found in the 1960s that electricity may be created illuminated organic dyes in electrochemical cells. Chlorophyll was isolated from spinach (photosynthesis) at the University of California in Berkeley. In 1972, the first chlorophyll-sensitized zinc oxide (ZnO) electrode was made. For the first time, photons were transformed into electricity by injecting electrons from excited dye molecules into a semiconductor with a wide band gap.[1]. ZnO-single crystals have been the subject of a lot of research.[2]However, the dye-sensitized solar cells' efficiency was poor, since the monolayer of dye molecules could only absorb around 1% of incident light. As a consequence, the efficiency was improved by improving the porosity of the fine oxide powder electrode, which increased dye absorption over the electrode and, as a result, increased light harvesting efficiency (LHE). Nano porous titanium dioxide (TiO<sub>2</sub>) electrodes with a rough factor of around ca.1000 were discovered as a result, and DSSCs with a 7 percent efficiency were created in 1991. [3] Such cells, also known as Grätzel cells, were co-invented by Michael Grätzel Brian O'Regan and at UC Berkeley in 1988 and [3] further developed by the same scientists at EPFL (Ecole Polytechniques Federale de Lausanne) until 1991. Michael Grätzel and Brian O'Regan and created a device based on a 10-µm-thick, high-surface-area, optically transparent TiO<sub>2</sub> nanoparticle film that was sensitised for light harvesting with a monolayer of a charge transfer dye with ideal spectral characteristics. The device harvested 46% of the incident solar energy flow and had extremely high efficiency, even exceeding 80% for the conversion of

incident photons to electrical current. In simulated solar light, the overall incident photon to current conversion efficiency (IPCE) yield was 7.1-7.9%, while in diffuse daylight, it was 12%. The practical use was made possible by a substantial short circuit current density  $J_{sc}$  (more than 12 mA/cm<sup>2</sup>), outstanding stability (at least five million turnovers without decomposition), and cheap cost.[3] Grätzel et al. reported a 9.6% cell efficiency in 1993, and then a 10% efficiency in 1997 at the National Renewable Energy Laboratory (NREL). As stable adsorption onto the semiconductor substrate, sensitizers are commonly constructed with functional groups such as -COOH, -PO<sub>3</sub>H<sub>2</sub>, and -B(OH)<sub>2</sub>. [4,5] Costa et al. reported an efficiency of 8.75 percent for hybrid dye-titania nanoparticle-based DSSC for enhanced low temperature performance in 2018.[6] Si has two purposes in a conventional solar cell: it operates as a source of photoelectrons and it producing an electric field to separate the charges and produce a current. In DSSCs, however, the bulk of the semiconductor is only utilized as a charge transporter, with photosensitive dyes providing the photoelectrons. The power conversion efficiency (PCE) of DSSCs was theoretically projected to be about 20% [7,8] As a result, substantial research has been conducted on DSSCs over the years in order to increase their efficiency and commercialisation. However, throughout the last few decades, numerous studies have been conducted to increase the performance of DSSCs. For example, if one examines the review articles or papers published between 1920 and 1921, one may see a significant change in the performance and construction of these cells. A few review papers are addressed below, with the purpose and primary results displayed in each article to get an understanding of how the performance of these cells has been enhanced and, as a consequence, how DSSCs became a hot issue for researchers.

Anandan reviewed the advancements and emerging problems in dye-sensitized solar cells up to 2007.[9] Light harvesting inorganic dye molecules, p-CuO nanorod counter electrodes, and self-organization of electro active polymers were the primary components of his review work, and he demonstrated how these materials behave in a rationally constructed solar cell. The maximum IPCE, on the other hand, is

In the review paper on naphthyridine, 7% was examined. Ru complex that is well-coordinated [10] this was satisfactory until 2007, but pales in comparison

to the efficiency shown in later research. The present status and advances in the field of photo electrode, photosensitizer, and electrolyte for DSSCs till 2015 were the major focus of the review paper published by Bose et al. [11] they included an intriguing study that compared the performance of the DSSC module to that of the Si-based module using the graph presented in Fig. 1 [12], concluding that the DSSC module's performance is considerably superior to that of the Si module. In addition, the maximum efficiency stated in this review study for N719 dye-based DSS was 11.2 per cent.

Sensitizers, such as ruthenium complexes metal-free organic dyes, quantum dot sensitizer, perovskite-based sensitizer, mordant dyes, and natural dyes, were highlighted by Shalini et al. [13]. However, while this article covers a lot of knowledge about to different types of sensitizers, it leaves out information on other important DSSC components. Apart from covering all of the many components of DSSCs, Jihuai Wu et al. [14] focused on the counter electrode element of the device. They spoke about studying several forms of counter electrodes based on transparency and and flexibility, metals and alloys, carbon materials, conductive polymers, transition metal complexes, and hybrids. In the review paper, the maximum efficiency of 14.3 percent was described for the DSSC fabricated with Au/GNP as a counter electrode, Co as a redox couple, and LEG4 + ADEKA-1 as a sensitizer [15]. Similarly, Yeoh et al. and Fan et al. [16, 17] have provided a brief overview of the DSSC photoanode. They divided photoanode modification into three categories: interfacial modification such as through blocking and scattering layers, compositing, doping with non-metallic anions and metallic cations, interfacial engineering, and replacing conventional mesoporous semiconducting metal oxide films with 1-D or 2-D nanostructures.

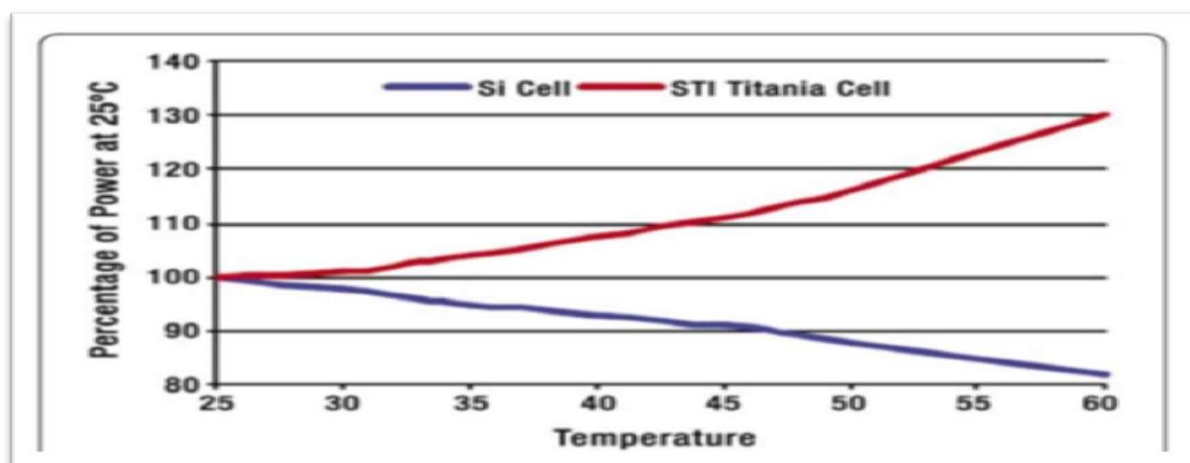


**FIG.1 THE PERFORMANCE OF DYE PV MODULES INCREASES WITH TEMPERATURE,  
CONTRARY TO S-BASED MODULES**

## **Construction and working of DSSCs**

A DSSC's four key parameters are the working electrode, sensitizer (dye), redox-mediator (electrolyte), and counter electrode. DSSC is a combination of a working electrode soaked in a sensitizer or dye and a counter electrode soaked in a thin layer of electrolyte bound together with a hot melt tape to prevent electrolyte leakage (as shown in Fig. 2). The components of DSSCs, as well as their construction and operation, are describe below.

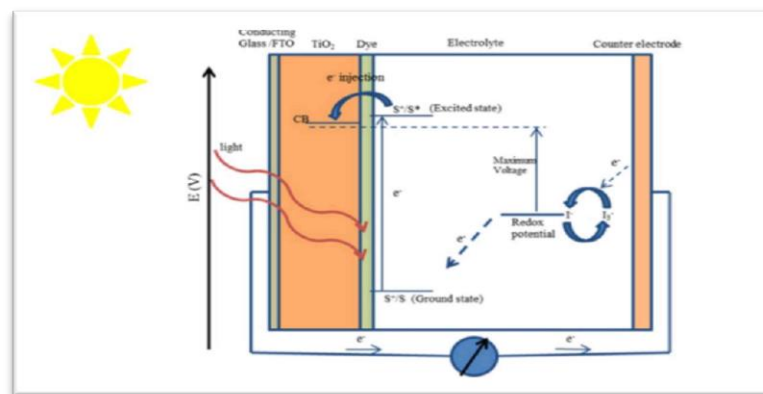


**FIG. 2 CONSTRUCTION AND WORKING PRINCIPLE OF THE DYE-SENSITIZED  
NANOCRYSTALLINE SOLAR CELLS**

The main components of DSSCs are

- I. Transparent and Conductive Substrate
- II. Working Electrode
- III. Photosensitizer or Dye
- IV. Electrolyte
- V. Counter
- VI. Electrode

### **I. TRANSPARENT AND CONDUCTIVE SUBSTRATE**

DSSCs are usually made up of two sheets of conduction-transparent materials that serve as a substrate for the deposition of the semiconductor and catalyst

while simultaneously acting as current collectors [18, 19] The following are the features of a substrate utilised in a DSSC:

To begin with, the substrate must have more than 80% transparency in order for optimal sunlight to reach the cell's effective area. Second, it should have a high electrical conductivity for efficient charge transfer and low energy loss in DSSCs. Indium-doped tin oxide (ITO,  $\text{In}_2\text{O}_3 \cdot \text{Sn}$ ) and fluorine-doped tin oxide (FTO,  $\text{SnO}_2 \cdot \text{F}$ ) are commonly used as conductive substrates in DSSCs. Soda lime glass is covered with layers of indium-doped tin oxide and fluorine doped tin oxide to create these substrates. ITO films have a transmittance of  $> 80\%$  and a sheet resistance of  $18 \text{ Q/cm}^2$ , whereas FTO films have a lower transmittance of 75% in the visible area and a sheet resistance of  $8.5 \text{ Q/cm}^2$ .

## **II. WORKING ELECTRODE (WE)**

The working electrodes (WE) are formed by depositing a thin layer of oxide semiconducting materials over a clear conducting glass plate composed of FTO or ITO, such as  $\text{TiO}_2$ ,  $\text{Nb}_2\text{O}_5$ ,  $\text{ZnO}$ ,  $\text{SnO}_2$ , and  $\text{NiO}$  (n-type) and  $\text{NiO}$  (p-type). The energy band gap of these oxides ranges from 3-3.2 eV. Although alternative wide band gap oxides such as  $\text{ZnO}$  and  $\text{Nb}_2\text{O}_5$  have also shown promise in DSSCs [22,23] the application of an anatase allotropic form of  $\text{TiO}_2$  is more commendable in DSSCs than the rutile form due to its higher energy band gap of 3.2 eV versus the rutile form's band gap of about 3 eV [20,21]  $\text{TiO}_2$  is commonly employed as a semiconducting layer because it is non-toxic, inexpensive, and readily available. However, because these semiconducting layers absorb only a small fraction of UV light, these working electrodes are then immersed in a mixture of a photosensitive molecular sensitizer and a solvent. Following the soaking of the film in the dye solution, Covalent bonds form between the dye and the  $\text{TiO}_2$  surface. Because of the electrode's porous shape and vast surface area, a significant number of dye molecules adhere to the Nano crystalline  $\text{TiO}_2$  surface. As a result, light absorption rises at the semiconductor surface.

## **III. PHOTOSENSITIZER OR DYE**

Dye is the component of the DSSC that is responsible for the highest absorption of incident light, and any material that is dye should have the following photo physical and electrochemical properties:

- a) The dye must be luminous

- b) The dye's absorption spectra should include ultraviolet-visible (UV-vis) and near-infrared (NIR) wavelengths.
- c) The highest occupied molecular orbital (HOMO) should be placed far away from the surface of the TiO<sub>2</sub> conduction band, while the lowest unoccupied molecular orbital (LUMO) should be placed as close to the TiO<sub>2</sub> surface as possible, and thus should be higher in relation to the TiO<sub>2</sub> conduction band potential.
- d) The HOMO should be lower than the redox electrolyte value.
- e) To improve the long-term stability of cells, the dye's periphery should be hydrophobic, since this results in less direct contact between electrolyte and anode ; otherwise, water-induced dye distortion from the TiO<sub>2</sub> surface may develop, reducing cell stability.
- f) . To avoid the dye from aggregating on the TiO<sub>2</sub> surface, co-absorbents such as chenodeoxycholic acid (CDCA) and anchoring groups such as alkoxy-silyl [24] gthosphoric acid [25] and carboxylic acid group [26, 27] were placed between the dye and the TiO<sub>2</sub> surface.

As a result, dye aggregation is prevented, and the recombination process [28] between the redox electrolyte and electrons in the TiO<sub>2</sub> nanolayer is limited, as well as the development of stable linkage.

#### IV. ELECTROLYTE

An electrolyte (such as I/I<sub>3</sub>Br/Br<sub>2</sub> [29], SCN/SCN<sub>2</sub> [30], and Co(II)/Co(III) [31] has five main components, i.e., redox couple, solvent, additives, ionic liquids, and cations. The following properties should be present in an electrolyte:

- a) The redox couple must be able to efficiently regenerate the oxidised dye.
- b) Chemical, thermal, and electrochemical stability should be long-term.
- c) With DSSC components, it should be non-corrosive.
- d) Allows rapid dispersion of charge carriers, improves conductivity, and ensures effective contact between the working and counter electrodes.
- e) An electrolyte's absorption spectra should not overlap with a dye's absorption spectra.

Although I/I<sub>3</sub> has been shown to be a very efficient electrolyte [32], its use in DSSCs has certain drawbacks. I/I<sub>3</sub> electroyte corrodes glass and TiO<sub>2</sub>/Pt; it is

very volatile and causes photodegradation and dye desorption, as well as having poor long-term stability [33, 34]. Acetonitrile (ACN), N-methylpyrrolidine (NMP), and solvent mixes like ACN/valeronitrile have been employed as high-dielectric-constant solvents. TBP is primarily employed as an additive to push the conduction band of  $\text{TiO}_2$  upwards, resulting in a higher open circuit voltage ( $V_{oc}$ ), lower cell photocurrent  $I_{sc}$ , and lower injection driving force. Through reverse transfer to an electrolyte, TBP on a  $\text{TiO}_2$  surface is believed to reduce recombination [35]. . The major disadvantage of ionic liquids, however, is their leakage issue. As a result, solid-state electrolytes have been designed to overcome the disadvantages of ionic liquid (IL) electrolytes [36], Long-term light soaking studies on sealed cells have also developed significantly over the years to assess the failure of the redox electrolyte or the sealing under long-term illumination [37].

## V. COUNTER ELECTRODE (CE)

CE in DSSCs is usually made from platinum (Pt) or carbon (C). The working and counter electrodes are then sealed together, and an electrolyte is then filled using a syringe. The reduction of  $\text{I}^-/\text{I}_3^-$  liquid electrolyte is catalysed by the counter electrode, which collects holes from the hole transport materials (HTMs). Pt is mostly utilised as a counter electrode because of its better efficiency. [38], however because to its increased cost and scarcity, a substitute for Pt was urgently required. As a result, numerous alternatives have emerged to replace Pt in DSSCs, including carbon [39], carbonylsulfide (CoS) [40], Au/GNP [15], alloy CEs such FeSe [41], and  $\text{CoNi}_{0.25}$  [42], although Jihuai Wu et al. [14] discuss the various types of CEs.

## WORKING PRINCIPLE

- a) The incident light (photon) is absorbed by a photosensitizer, and electrons are promoted from the ground state ( $S^+/S$ ) to the excited state ( $S^+/S^*$ ) of the dye as a result of the photon absorption. The absorption for most dyes is in the range of 700 nm, which corresponds to photon energy of almost 1.72 eV.
- b) Now, excited electrons with nanosecond lifetimes are injected into the conduction band of nanoporous  $\text{TiO}_2$ , an electrode that falls below the dye's excited state and absorbs a tiny percentage of solar photons from the UV area [43]. The dye oxidises as a result.

- c) The injected electrons travel between TiO<sub>2</sub> and nanoparticles before diffusing back to the back contact transparent conducting oxide (TCO). Electrons reach the counter electrode through the external circuit.
- d) Electrons at the counter electrode reduce I<sub>3</sub> to I<sup>-</sup>; resulting in dye regeneration or regeneration of the dye's ground state due to electron acceptance from the I ion redox mediator, and I is oxidised to I<sup>+</sup>. (oxidized state)
- e) The oxidised mediator (I<sub>3</sub><sup>+</sup>) diffuses back to the counter electrode and is reduced to I ion.

## EVALUATION OF DYE-SENSITIZED SOLAR CELL PERFORMANCE

The performance of a dye-sensitized solar cell can be evaluated using incident photon to current conversion efficiency (IPCE, per cent), short circuit current  $j_{sc}$ , mAcm<sup>-2</sup>), open circuit voltage ( $V_{oc}$  V), maximum power output [ $P_{max}$ ], overall efficiency [ $\eta$ , percent], and fill factor [FF] (as shown in Fig. 3) at a constant light level exposure as shown in Eq. 1 for a constant light level exposure[44].

When the negative and positive electrodes of a cell are short circuited at a zero mV voltage, current is produced. The potential difference between the conduction band energy of semiconducting material and the redox potential of electrolyte is defined as  $V_{oc}$  (V) across negative and positive electrodes in open circuit at zero milliampere (mA) current.  $P_{max}$  is the DSSC's maximum efficiency in converting sunlight into electricity. FF is the ratio of the maximum power output ( $j_{mp} \times V_{mp}$ ) and the product ( $V_{oc} \times J_{sc}$ ).

$$FF = \frac{\text{Area A}}{\text{Area B}} = \frac{j_{mp} \times V_{mp}}{J_{sc} \times V_{oc}}$$

Also, the total efficiency (percent) is the percentage of solar energy (shining on a photovoltaic [PV] device) converted into electrical energy, where  $\eta$  grows as  $J_{sc}$  decreases and  $V_{oc}$  FF and molar coefficient of dye increase, accordingly.

$$\eta(\%) = \frac{j_{sc} \times V_{oc} \times FF}{P_{in}} \quad \dots \dots 1)$$

The ratio of the number of electrons flowing through the external circuit to the number of photons incident on the circuit is known as external quantum efficiency (also known as IPCE). At any wavelength  $\lambda$ , cells surface. It is given as follows

$$\text{IPCE}\%(\lambda) = 1240 \times \frac{J_{sc}}{P_{in} \lambda} \quad \dots\dots 2)$$

IPCE values are also related to LHE,  $\phi_{E1}$ , and  $\eta_{EC}$ . As Shown in Eq. 3 [45],

$$\text{IPCE}(\lambda, \text{nm}) = \text{LHE}\phi_{E1}\eta_{EC} \quad (3) \quad \dots\dots 3)$$

where LHE is the light harvesting efficiency,  $\phi_{E1}$  is electron injection quantum efficiency, and  $\eta_{EC}$  is the efficiency of collecting electrons in the external circuit

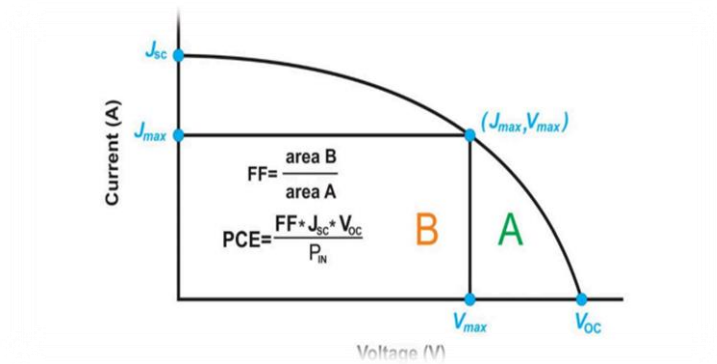


Fig. 3 I-V curve to evaluate the cells performance

## VARIOUS TECHNIQUES FOR INCREASING THE EFFICIENCY OF DSSCS

To increase the efficiency and stability of DSSCs, the focus must be on fundamental fabrication processes and materials, as well as how these systems function. Few techniques to enhance the efficiency of solar cells are briefly described below:

1. By depositing a homogeneous thin layer or under layer of  $\text{TiO}_2$  nanoparticles over the conduction glass plate, the development of the dark current is reduced or prevented. As a result, the electrolyte does not make direct contact with the FTO or back contact, and as a result, the collector electrons do not decrease the electrolyte, limiting the generation of dark current.
2. Co-sensitization is another way to optimize the Performance of DSSC. In co-sensitization, two or more sensitizing dyes with different absorption spectrum ranges are mixed together to broaden the spectrum response range [46]

3. By inserting phosphorescence or luminescence chromophores, such as applying rare-earth doped oxides into the DSSC [47-49], coating luminescent layer on the glass of the photoanode [50-51] i.e., using plasmonic phenomenon [52] and adding energy relay dyes (ERDs) to the electrolyte [53, 54, 55].
4. By using various types of materials in the manufacturing of electrodes like nanotubes, nanowires, graphene etc., the efficiency of these cells can be increased.
5. The efficiency of DSSC can also be increased by using various types of electrolytes instead of a liquid one like gel electrolyte and quasi-solid electrolytes.
6. The careful pre and post treatment of the working electrode like anodization pre-treatment and  $\text{TiCl}_4$  treatment is also very useful in increasing the efficiency of DSSC [14].
7. By developing hydrophobic sensitizers, the performance as well as the efficiency of these cells can be strongly improved

### Previous And Future Improvements in DSSCs,

New materials that are light weight, thin, low cost, and easy to synthesis are needed to build low cost, more flexible, and stable DSSCs with higher efficiencies.

As a result, this section covers both historical and future advancements in the field of DSSCs. This section provides a summary of the work done by several researchers during the previous 10-12 years, as well as the results they have discovered for various cells.

### **COUNTER ELECTRODES AND WORKING**

Grätzel and co-worker, the performance of DSSCs was dramatically improved At EPFL [3, 26], they demonstrated efficiency of 7-10% under AM 1.5 irradiation using a novel Ru bipyridyl complex as a sensitizer and an ionic redox electrolyte, as well as a nanocrystalline  $\text{nc-TiO}_2$  thin-film electrode with nanoporous structure and large surface area. The conduction band level of  $\text{TiO}_2$  electrode, and the redox potential of  $\text{I}^-/\text{I}_3^-$  have been assessed as -0.7 V versus saturated calomel electrode (SCE) and 0.2 V versus SCE [56,57]. In 2014 [58], a binary oxide photoelectrode was developed using coffee as a natural dye. When DSSCs with graphite-P25 composites as photo anodes were compared to P25 alone, Hu et al. found that the performance of the DSSCs

with graphite-P25 composites as photo anodes was 30 percent better. Apart from Titanium dioxide, ( $\text{TiO}_2$ ) carbon and its various allotropes are frequently used in DSSCs to fulfill future demand and have emerged as an ideal surrogate material for DSSC. According to several studies, including hydrothermal or chemical synthesis of carbon nanotubes (CNTs) in  $\text{TiO}_2$  The performance of the cell was considerably enhanced using sol-gel techniques [59-61] Aside from  $\text{TiO}_2$ , carbon and its many form To meet future demand, allotropes are widely used in DSSCs and have emerged as a perfect substitute material for the DSSC According to several studies, including hydrothermal or chemical synthesis of carbon nanotubes (CNTs) in  $\text{TiO}_2$  The performance of the cell was greatly improved using sol-gel techniques According to Sun et al., DSSCs with graphene in  $\text{TiO}_2$  photoanode had a PCE of 4.28 percent, which was 59 percent greater than those without graphene.[62] Sharma et al. [63] demonstrated that employing modified  $\text{TiO}_2$  (G- $\text{TiO}_2$ ) photoanode instead of pure  $\text{TiO}_2$  photoanode improved the PCE value of the co-sensitized solar cell from 7.35 to 8.15 percent. The electrically and catalytically functioning carbon fabric was proven to operate as a permeable and flexible counter electrode for DSSC in 2014 [64]. The TiN nanotube arrays and TiN nanoparticles supported on carbon nanotubes demonstrated strong electrocatalytic activity for the reduction of triiodide ions in DSSCs, according to the researchers [65,66]. Sun et al. used single-crystal  $\text{CoSe}_2$  nanorods as an efficient electrocatalyst for DSSCs in 2014 [67].

Calogero et al. created a transparent and low-cost counter electrode using platinum nanoparticles prepared from the bottom up. They showed that the observed solar energy conversion efficiency with such a cathode was the same as that obtained with a platinum-sputtered counter electrode and even exceeded 50% with a standard electrode generated by chlorine platinum acid thermal decomposition in similar working conditions [68]. They improved the performance of a counter electrode based on platinum sputtering by 4.75 percent under  $100 \text{ mWcm}^{-2}$  (AM 1.5) of simulated sunshine by employing an unique back-reflecting layer of silver. They found that the platinum nanoparticle-based cathode electrode (CE) prepared by Pt sputtering deposition method appeared more transparent than the platinum CE prepared by Pt acid thermal decomposition method for optical transmittance at different wavelengths of platinum-based films, i.e., Pt nanoparticles, Pt thermal

decomposition, and Pt sputtered deposited onto FTO glass. However, when using the Pt nanoparticle deposition technique, the transmittance was very poor (as shown in Fig. 4).

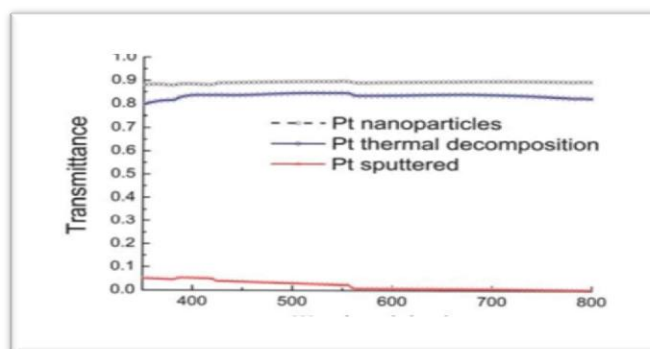


**FIG 4 OPTICAL TRANSMITTANCE OF PLATINUM-BASED FILMS**

(Pt nanoparticles, Pt thermal decomposition, Pt sputtered) deposited onto FTO glass)

DSSCs using zirconia-doped  $\text{TiO}_2$ , nanoparticle, and nanowire composite photoanode films were described by Maheswari et al. They found that the combination of a zirconia-doped photoanode with a hafnium oxide ( $\text{HfO}_2$ ) blocking layer results in the highest  $\eta = 9.93$  percent, and that the combination of a zirconia-doped photoanode with a blocking layer effectively restrains the recombination process and increases the PCE of the DSSCs [69]. Many concepts, on the other hand, do not attain high efficiency right away, but they do incorporate many ideas and elements for the synthesis of new materials. Shejale et al., for example, obtained a  $\eta = 1.98$  percent for DSSC employing carbon-coated stainless steel as a CE (97). In 2018, a study was conducted to determine the effect of microwave exposure on photoanode efficiency, and it was discovered that the cell's efficiency increased after exposure. A Lil electrolyte, Pt cathode,  $\text{TiO}_2$  photoanode, and Alizarin red as a natural sensitizer were utilised to make the DSSC. The cell had an efficiency of 0.144 percent when the photoanode was exposed to microwaves for 10 minutes [70]. Similarly, as previously noted, various materials are synthesised as CE for efficient DSSCs. Guo et al. synthesised an  $\text{In}_{2.77}\text{S}_4$ @conductive carbon ( $\text{In}_{2.77}\text{S}_4$ @CCP hybrid CE via a two-step method last year and achieved  $\eta = 8.71$  percent for the DSSC with superior electrocatalytic activity for the reduction of triiodide, that was also comparable to the commercial Pt-based DSSC that showed PCE of 8.75 percent, respectively [71]. Tsai et al. examined the doping of an organic acid, 1S-(+)-camphorsulfonic acid, with the conductive polymer polyfo-methoxyaniline) to form a hybrid (CSAPOMA) and its use in

DSSCs as CE. Surface roughness, impedance, and crystallinity were all increased with this CE [72]. Liu et al. [73] developed DSSCs with  $\text{Co}(\text{bpy})_3^{3+/2+}$  as the redox couple and carbon black (CB) as the CE in 2017. The electrocatalytic activity of a well-prepared CB film was found to be superior to that of standard sputtered Pt.  $\text{Cu}_2\text{O}$  has also been used as a CE in DSSC [74] due to the flexibility of Cu foil substrates. [74] has reported the fabrication of various samples by varying the sintering temperature of the CEs and achieving a maximum efficiency of 3.62 percent at 600 °C. The V characteristics and IPCE curves of DSSCs using various  $\text{Cu}_2\text{O}$  CEs are shown in Figure 5

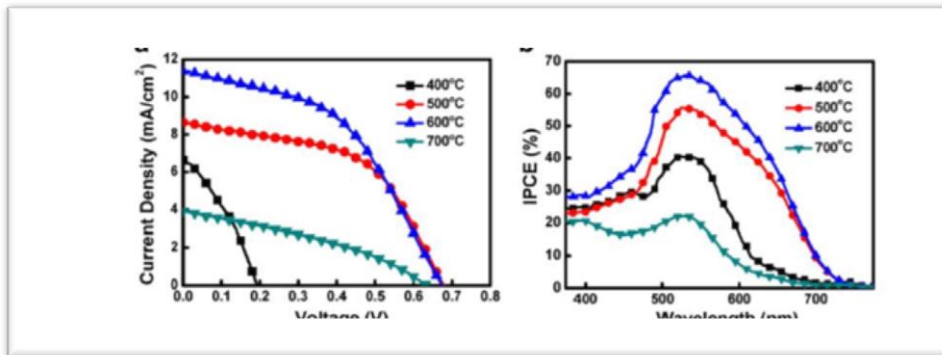


Fig 5 The a current density-voltage (J-V) and b incident monochromatic photon-to-current conversion efficiency (IPCE) Curves of DSSCs using various  $\text{Cu}_2\text{O}$  CE [102]

In 2013, an increase in the value of FF and  $\eta$  was discovered by replacing the FTO with Mo as the counter electrode conductor [75]. Due to the dissimilarity of the sheet resistance between FTO (8.2  $\Omega/\text{sq}$ ) and Mo (0.16  $\Omega/\text{sq}$ ), the EIS Nyquist plots (as shown in Fig 6)

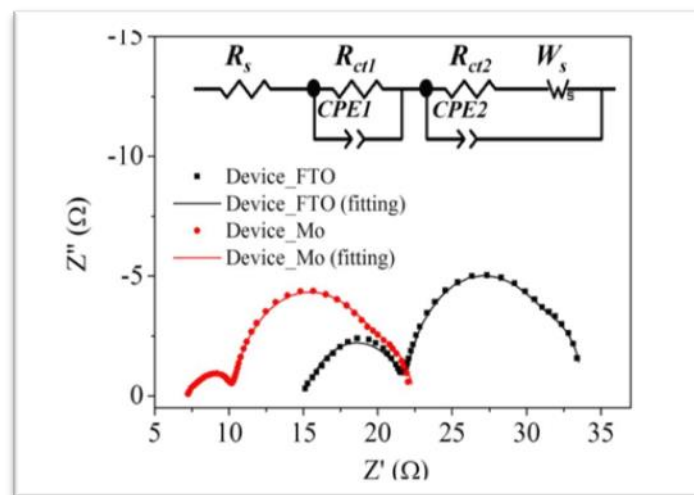


Fig 6 Nyquist plots of the Device\_FTO and Device Mo. The inset indicates an equivalent circuit model used for the devices [103]

revealed a difference in  $R_s$  between the devices employed FTO ( $15.11 \Omega\text{cm}^2$ ) and Mo ( $7.25 \Omega\text{cm}^2$ ). The higher redox reactivity of Pt on Mo than on FTO resulted in a reduction in the  $R_{\text{ct1}}$  value from 6.87 to  $3.14 \Omega\text{cm}^2$  when FTO was replaced with Mo.

Maiiaugree et al. produced DSSCs using carbonised mangosteen peel (MPC) as a natural counter electrode and a mangosteen peel dye as a sensitizer in the process of developing new materials [76]. In carbonised mangosteen peels, they discovered a typical mesoporous honeycomb-like carbon structure with a rough nanoscale surface, achieving the greatest value of  $\eta = 2.63$  percent. They discovered a broad D-peak ( $130.6 \text{ cm}^{-1}$  of FWHM) at  $1350 \text{ cm}^{-1}$  indicating strong disorder of  $\text{sp}^3$  carbon, and a narrower G peak ( $68.8 \text{ cm}^{-1}$  of FWHM) at  $1595 \text{ cm}^{-1}$ , which correlated with a graphite oxide phase described in 2008 [77] by evaluating the Raman spectra (shown in Fig. 7).

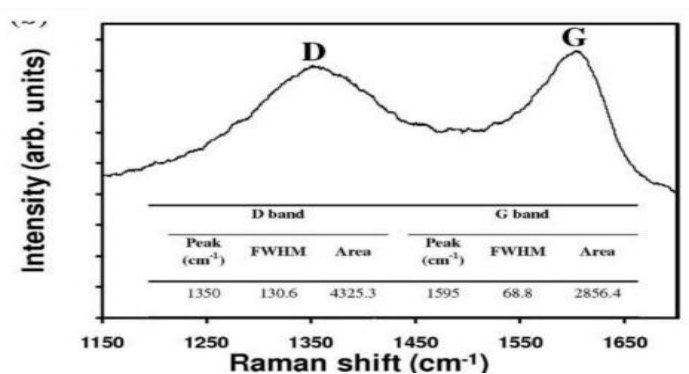


Fig. 7 Raman spectra of mangosteen peel carbon [104]

Thus, the graphite oxide from MPC was determined to be a highly organised  $\text{sp}^2$  hexagonal carbon oxide network. In addition, table 1 summarises the I-V characteristics of DSSCs using various WE and CE.

| WE/CE  | $V_{OC}$ (mV) | $J_{SC}$ ( $\text{mAcm}^{-2}$ ) | FF (%) | $\eta$ (%) |
|--|---------------|---------------------------------|--------|------------|
| WE: TiO <sub>2</sub> doped with tungsten                                   | 730           | 15.10                           | 67     | 7.42       |
| WE: TiO <sub>2</sub> doped with scandium                                   | 752           | 19.10                           | 68     | 9.60       |
| WE: TiO <sub>2</sub> doped with indium                                     | 716           | 16.97                           | 61     | 7.48       |
| WE: TiO <sub>2</sub> doped with boron                                      | 660           | 7.85                            | 66     | 3.44       |
| WE: TiO <sub>2</sub> doped with fluorine                                   | 754           | 11                              | 76     | 6.31       |
| WE: TiO <sub>2</sub> doped with carbon                                     | 730           | 20.38                           | 57     | 8.55       |
| WE: ONT/FTO  | 700           | 10.65                           | 70     | 5.32       |
| WE: G-TiO <sub>2</sub> NPs/TiO <sub>2</sub> NTs                            | 690           | 16.59                           | 56     | 6.29       |
| WE: TiO <sub>2</sub> doped with Cu   | 591           | 6.84                            | 56     | 2.28       |
| WE: 7.5% SnO <sub>2</sub> doped TiO <sub>2</sub>                           | 790           | 14.53                           | 58     | 6.7        |
| WE: TiO <sub>2</sub> :Y <sub>1.86</sub> Eu <sub>0.14</sub> WO <sub>6</sub> | 757           | 12.3                            | 43     | 3.9        |
| WE: Nb <sub>2</sub> O <sub>5</sub>   | 738           | 6.23                            | 68.3   | 3.15       |
| WE: Nanographite-TiO <sub>2</sub>  | 720           | 1.69                            | 35     | 0.44       |
| CE: PtCo   | 717           | 16.96                           | 66     | 7.64       |
| CE: Pt+SLGO  | 670           | 7.9                             | 65     | 3.4        |
| CE: PtMo   | 697           | 15.48                           | 62     | 6.75       |
| CE: PtC <sub>0.05</sub>  | 739           | 13.07                           | 71     | 6.88       |
| CE: CoNi <sub>0.25</sub>   | 706           | 18.02                           | 66     | 8.39       |
| CE: Ni-PANI-G  | 719           | 11.56                           | 64     | 5.32       |
| CE: PANI nanoribbons   | 720           | 17.92                           | 56     | 7.23       |
| CE: Pd <sub>17</sub> Se <sub>15</sub>                                      | 700           | 16.32                           | 65     | 7.45       |
| CE: PtCuNi   | 758           | 18.30                           | 69     | 9.66       |
| CE: g-C <sub>3</sub> N <sub>4</sub> /G                                     | 723           | 14.91                           | 66     | 7.13       |
| CE: FeN/N-doped graphene   | 740           | 18.83                           | 78     | 10.86      |
| CE: MoS <sub>2</sub> nanofilm  | 740           | 16.96                           | 66     | 8.28       |
| CE: Ni <sub>0.33</sub> Co <sub>0.67</sub> Se microsphere                   | 789           | 17.29                           | 67     | 9.01       |
| CE: Tubular orthorhombic CoSe <sub>2</sub>                                 | 771           | 17.35                           | 70     | 9.34       |
| CE: CoSe <sub>2</sub>  | 809           | 17.65                           | 71     | 10.17      |
| CE: In <sub>2.77</sub> S <sub>4</sub> @CC                                  | 750           | 17.34                           | 67     | 8.71       |
| CE: Electrochemically deposited Pt   | 750           | 17.16                           | 60     | 7.72       |
| CE: Fe <sub>3</sub> O <sub>4</sub> @RGO-NMCC                               | 760           | 17.00                           | 70     | 9.04       |
| CE: CB-NPs/s-PT  | 764           | 17.21                           | 69     | 9.02       |
| CE: AC/MWCNTs  | 753           | 16.07                           | 83     | 10.05      |
| CE: NiCo <sub>2</sub> S <sub>4</sub>                                       | 148.6         | 2.98                            | 55.8   | 0.24       |
| CE: SS:Graphene  | 524           | 1.46                            | 26     | 1.98       |
| CE: Ru <sub>0.33</sub> Se  | 722           | 17.86                           | 67.9   | 8.76       |
| CE: 5% Ag-doped SnS <sub>2</sub>   | 740           | 16.7                            | 70     | 8.70       |
| CE: Cu <sub>2</sub> O  | 680           | 11.35                           | 47     | 3.62       |

Table 1 Photovoltaic parameters of DSSCs employing different types of WEs and CE

## 2. CHAPTER

### ELECTROLYTE

Different electrolytes, such as gel electrolytes, quasi-solid-state electrolytes, ionic liquid electrolytes, and others, have been used as mediators to improve and research the performance of DSSCs so far. Adding energy relay dyes to the electrolyte, on the other hand, has started a new trend to improve the performance of DSSCs.

#### 1). LIQUID ELECTROLYTE

Iodide/triiodide redox couple and high dielectric constant organic solvents like ACN, 3-methoxypropionitrile (MePN), propylene carbonate (PC),  $\gamma$ -butyrolactone (GBL), N-methyl-2-pyrrolidone (NMP), ethylene carbonate (EC), and counter ions of iodides, where solvents are the key component of a liquid electrolyte, can improve the cells efficiency through. Organic solvents can be classified as imidazolium, < picolinium, < alkylpyridinium based on their stability. Among the many solvent properties such as donor number, dielectric constants, and viscosity, the donor number has a significant impact on the  $V_{oc}$  and  $J_{sc}$  of DSSCs. The cell performance is greatly improved by adding a tiny amount of electric additives such as N-methylbenzimidazole (NMBI), guanidinium thiocyanate (GuSCN), and TBP. A coab sorbent, like solvents, plays an important role in the functioning and performance of an electrolyte. Organic solvents can be classified as imidazolium, < picolinium, < alkylpyridinium based on their stability. Among the many solvent properties such as donor number, dielectric constants, and viscosity, the donor number has a significant impact on the  $V_{oc}$  and  $J_{sc}$  of DSSCs. The cell performance is greatly improved by adding a tiny amount of electric additives such as N-methylbenzimidazole (NMBI), guanidinium thiocyanate (GuSCN), and TBP. A coab sorbent, like solvents, plays an important role in the functioning and performance of an electrolyte. The addition of coabsorbents to an electrolyte reduces charge recombination between photoelectrons in the semiconductor and the electrolyte's redox shuttle. Second, a coabsorbent dicing may change the position of the band edge of the  $TiO_2$ -conduction band, resulting in an increase in the cell's  $V_{oc}$  value. This prevents dye aggregation on the  $TiO_2$  surface, resulting in the cell's long-term stability and a rise in  $V_{oc}$ . Despite the fact that iodide/triiodide as a redox pair for a liquid electrolyte

has the best regeneration of the oxidised dye, its feature of severe corrosion for many sealing materials results in poor long-term durability of the DSSC. For iodide/as a redox couple for a liquid electrolyte, regeneration of the oxidised dye is seen; nevertheless, its feature of severe corrosion for many sealing materials leads in poor long-term durability of the DSSC.

In a liquid electrolyte, ionic liquids (IL) or room temperature ionic liquids (RTIL) act as a stand-in for organic solvents. Despite their many advantages, including as low flammability, high electrical conductivity at room temperature (RT), and a large electrochemical window, they are less suitable for DSSCs. The reduced transport speed of iodide/triiodide in solvent-free IL electrolytes limits the restoration of oxidised dye due to their higher viscosity. Thus, by altering the  $\text{TiO}_2$  dye interface, i.e., by lowering the vapour pressure of the electrolyte's solvent, the performance of dye-sensitized solar cells can be improved.

In 2017, Puspitasari et al. investigated the effect of mixing dyes and solvent in electrolyte and fabricated a variety of devices as a result. For assessing the lifetime of DSSC, they employed two types of gel electrolyte based on PEG that were blended with liquid electrolyte. They also improved the efficiency of the electrolyte type II by using different solvents such as distilled water (type 1) and ACN (type I) with the addition of KI and iodine concentrations [78].

## **2). SOLID-STATE ELECTROLYTE (SSE)**

(SSE) is a solid electron-insulating material and ionic conductor and it is the characteristic component of the solid-state battery. It is used for electrical energy storage (EES) as a liquid electrolyte replacement, particularly in lithium-ion batteries. And advantages is that absolute safety, no harmful organic solvent leakage issues, low flammability, non-volatility, mechanical and thermal stability, easy processability, low self-discharge, higher attainable power density, and cyclability are the key benefits. This allows the use of a lithium metal anode in a practical device.

The SSE is divided into two categories

- A. Hole Transport Materials
- B. SSE Containing Iodide/Triiodide Redox Couple

**A.) HOLE TRANSPORT MATERIALS** :- (HTMs) are solid-state electrolytes, which means they are utilised as a medium. Because iodine/iodide electrolytes are very chemically aggressive by nature and easily erode other materials, especially metals, these materials have set a significant milestone in DSSCs and are successfully applicable in cells. Although the results are still unmatched with those obtained for iodine/iodide redox electrolytes due to the following rationale, most HTMs are chemically less aggressive inorganic solids, organic polymers, or p-conducting molecules.

- i) The high frequencies of charge recombination from  $\text{TiO}_2$ , to HTMs
- ii) Incomplete penetration of solid HTMs within a nanoporous  $\text{TiO}_2$ -layer results in poor electronic interaction between HTMs and the dye due to their solid nature. As a result, dye regeneration is incomplete.
- iii) HTM result in a drop in  $V_{oc}$  because the recombination rate of electrons in CB with HTM is higher than in iodine/iodide redox electrolytes.
- iv) The addition of organic hole conducting molecules raises the cell's series resistance because organic HTMs have lower hole mobility than IL electrolytes.
- v) Low intrinsic conductivities of HTMs.

### **B.) SSE CONTAINING IODIDE/TRIIODIDE REDOX COUPLE**

The interfacial contact properties of these solid-state electrolytes are better than those of HTMs, they have a wider range of applications. The fabrication of a DSSC based on solid-state electrolyte was reported, with an overall light-to-electricity conversion efficiency of 4.2 percent for the cell under irradiation of AM 1.5100  $\text{mWcm}^{-2}$  [79]

### **3.) QUASI-SOLID-STATE ELECTROLYTE (QSSE)**

QSSE is made up of a polymer host network swelled with liquid electrolytes, it has a hybrid network structure that exhibits both solid (cohesive property) and liquid (diffusive transport property) properties at the same time. Thus, ILs such as 1-propargyl-3-methylimidazolium iodide, bis(imidazolium) iodides, 1-ethyl-1-methylpyrrolidinium and polymer gel-like PEO, and polyvinylidene fluoride) and polyvinyl acetate containing redox couples are

commonly used as QSSEs to overcome the volatilization and leakage problems of liquid electrolytes [80,81], Sun et al. fabricated a DSSC using a wet-laid polyethylene terephthalate (PET) membrane electrolyte in 2015. PET is a textile fibre utilised as a matrix for an electrolyte in the form of a wet-laid non-woven fabric. According to their findings, this membrane can absorb electrolyte more efficiently, forming a quasi-solid that provides excellent interfacial contact between the DSSC and DSSC electrodes, preventing a short circuit. At 100 mWcm, the PCE of the quasi-solid-state DSSC assembled with an optimised membrane was 10.248 percent. They plasmatreated the membrane separately with argon and oxygen to increase the absorbance, which resulted in the electrolyte being retained, preventing evaporation, and a 15 percent longer lifetime of the DSSC compared to liquid electrolyte [82]. Figure 8 shows the polarization curves of DSSCs with various electrolytes under simulated AM 1.5 global sunlight (1 Sun, 100 mWcm<sup>-2</sup>)

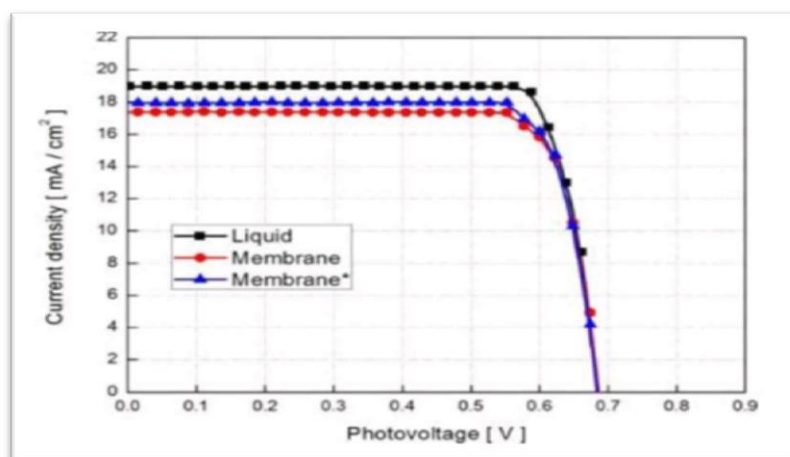
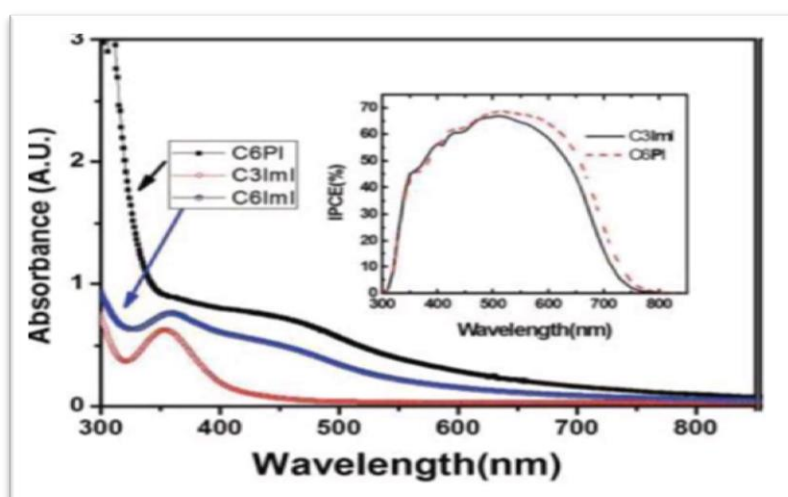


FIG 8 POLARIZATION CURVES OF DSSCs WITH VARIOUS ELECTROLYTES UNDER SIMULATED AM 1.5 GLOBAL SUNLIGHT (1 SUN 100 MWCM<sup>-2</sup>)[138]

## HOLE-CONDUCTING POLYMERS

For pure organic solar cells, an IPCE of 3.5 percent was attained by using a C60/polythiophene derivative in DSSCs [83]. However, this field is progressing slowly because solid polymer does not penetrate the TiO<sub>2</sub>, nanoporous layer, making deposition by traditional methods (such as CBD) difficult. As a result, just a few groups are used in DSSCs as conducting polymers. Using a fluorene-thiophene copolymer, Ravirajan et al. established a monochromatic efficiency of 1.4 percent at 440 nm.[84]. Researchers have been working hard to develop new electrolyte materials. According to Jeon et al., adding alkylpyridinium iodide ions to electrolytes improved the performance of dye-sensitized solar

cells. They observed that the cell using EC6PI (pyridinium salts) had better J-V characteristics, with 7.92 percent efficiency with  $V_{oc}=0.696$  V,  $J_{sc} = 17.74$  mA/cm, and  $FF= 0.641$ , as opposed to EC3ImI (imidazolium salts), which had = 7.46 percent with  $V_{oc}= 0.686$  V,  $J_{sc} = 16.99$  mA/cm, and  $FF= 0.64$  [85] They added UV spectra for C6ImI as a comparison and observed that the higher quantum efficiencies from the cell with EC6PI were obtained throughout a wide range of wavelengths from 460 to 800 nm The quantum efficiencies were virtually identical in the shorter wavelength range, which could be attributable to C6PI's capacity to absorb more incident light than C3ImI at shorter wavelengths. Despite this, the absorption coefficients for C6PI were higher than those for C6ImI throughout the whole range, but the cell efficiencies were very similar (as shown in Fig. 11). [85]



**Fig 9 UV-vis spectroscopy selected pyridinium and imidazolium salts. The inset is the IPCE data for the cells with EC3ImI and EC6PI, which are the best cells among each series [85]**

Lee et al. created and used conjugated polymer electrolytes (CPEs) having quaternized groups in polymer solution and gel electrolytes for DSSCs, such as MPF-E, MPCZ-E, MPCF-E, and MPCT-E. They discovered that when the polymer concentration in the electrolyte solution increased, the electrochemical impedance for cells based on CPE including polymer solution electrolytes increased as well, however PV performance decreased [86]. The FF and efficiencies for the DSSCs using various dyes and mediators are shown in Table 2.

| Dye              | Redox couple (RC)—(a)/HTM—(b)     | FF (%) | $\eta$ (%) |
|------------------|-----------------------------------|--------|------------|
| LEG4 + ADEKA-1   | (a) $\text{Co}^{3+/2+}$           | 77     | 14.3       |
| D358             | Tetra-n-propyl ammonium iodide    | 60     | 2.37       |
| N719             | (a) $\text{I}_3^-/\text{I}^-$     | 71     | 8.35       |
| Y123             | (a) $\text{Co}^{3+/2+}$           | 74     | 8.81       |
| EosinY           | (a) $\text{Co}(\text{bpy})_3$     | 72     | 3.85       |
| YD2-o-C8         | (a) $\text{Co}^{3+/2+}$           | 68     | 8.97       |
| Kojic acid-Azo 4 | (a) $\text{I}_3^-/\text{I}^-$     | 75     | 1.54       |
| N719             | (a) $\text{I}_3^-/\text{I}^-$     | 72     | 8.57       |
| N719             | (a) $\text{Co}^{3+/2+}$           | 71     | 10.42      |
| N719             | (a) $\text{I}_3^-/\text{I}^-$     | 67     | 7.88       |
| N719             | (a) $\text{I}_3^-/\text{I}^-$     | 72     | 9.96       |
| C106             | (a) $\text{T}_2^-/\text{T}^-$     | 70     | 7.60       |
| C106TBA          | (a) $\text{I}_3^-/\text{I}^-$     | 74     | 9.54       |
| YA422            | (a) $\text{Co}^{3+/2+}$           | 74     | 10.65      |
| SM315            | (a) $\text{Co}^{3+/2+}$           | 78     | 13         |
| Y123             | (a) $\text{Co}^{3+/2+}$           | 71     | 10.30      |
| Z907             | (a) $\text{T}_2^-/\text{T}^-$     | 72     | 7.90       |
| N3               | (a) $\text{I}_3^-/\text{I}^-$     | 71     | 9.25       |
| Y123             | (a) $\text{Co}^{3+/2+}$           | 78     | 9.90       |
| FNE29            | (a) $\text{Co}^{3+/2+}$           | 70     | 8.24       |
| CYC-B11          | (a) $\text{I}_3^-/\text{I}^-$     | 67     | 9          |
| 2-TPA-R          | (a) $\text{I}_3^-/\text{I}^-$     | 72     | 2.3        |
| T1               | (a) $\text{I}_3^-/\text{I}^-$     | 60     | 5.73       |
| PTZ-1            | (a) $\text{I}_3^-/\text{I}^-$     | 65.3   | 5.4        |
| Y123 (OD)        | (b) Spiro-OMeTAD                  | 76     | 7.2        |
| N719             | (b) VM3                           | 43     | 0.075      |
| Z907             | (b) AS37                          | 62     | 2.48       |
| N3               | (b) Pentacene                     | 49     | 0.8        |
| D102 (OD)        | (b) 4d                            | 32     | 0.54       |
| SQ (OD)          | (b) TVT                           | 64     | 0.19       |
| D102 (OD)        | (b) VMSC9                         | 38     | 0.47       |
| N719             | PET membrane                      | 83     | 10.24      |
| N719             | LC-5% doped                       | 61     | 4.61       |
| Mangosteen       | PEG: liquid electrolyte (Type I)  | 27     | 0.015      |
| Mangosteen       | PEG: liquid electrolyte (Type II) | 14.5   | 0.010      |

**TABLE 2 EFFICIENCIES FOR DIFFERENT DYES AND ELECTROLYTE**

### **3. CHAPTER DYES**

#### **DEVELOPMENTS IN DYE SYNTHESIS**

Dyes play such an important role in DSSCs,

1. Numerous inorganic organic
2. Metal-free dyes
3. Natural dyes

Likes N3 , N719 , N749 (black dye) , K19 , CYC-B11 , C101 , K8 , D102 , SQ, Y123, Z907 Mangosteen [78], and of them will be discussed below briefly:

#### **METAL COMPLEX**

Metal complexes are made up of a central metal atom or ion surrounded by several atom, which include atoms, ions, or molecules called ligands . Ligands are ions or molecules that can exist independently of the central metal atom or ion and are attached to it. Halide ions, carbon monoxide, ammonia, cyanide ion, and other ligands are examples.

Metal complex dyes made from heavy transition metals, such as ruthenium (Ru), osmium (Os), and iridium (Ir), have been widely used as inorganic dyes. dSSCs have been used in a variety of applications. Because of their extended excited lifetimes, highly efficient metal-to-ligand charge transfer spectrum, and strong redox characteristics, M is a metal, L is a ligand such as 2,2'-bipyridyl-4,4-dicarboxylic acid, and X is a halide, cyanide, thiocyanate, acetyl acetate, and thiocarbamate or water substituent group [87]. The ruthenium polypyridyl complexes show the best efficiencies and have been widely used because to their thermal and chemical stability and wide absorption spectrum from visible to near-infrared.

#### **RUTHENIUM (RU) COMPLEXES**

The black dye (ruthenium) [3]. They later reported an efficiency of roughly 10% using Ru-based dye (N749), which has given this problem a new perspective. Most Ru complexes are composed of Ru(II) atoms coordinated by polypyridyl ligands and thiocyanate moieties in octahedral geometry, and they have a moderate absorption coefficient of 18,000 M<sup>-1</sup> cm<sup>-1</sup> due to metal to

ligand charge transfer (MLCT) transitions. Ru (II) complexes cause the inter crossing of excited electrons into the long-lived triplet state, resulting in an increase in electron injection. Bipyridyl moieties can also be replaced by carboxylate polypyridine Ru dyes, phosphate Ru dyes, and poly nuclear bipyridyl Ru dyes to improve the absorption and emission of Ru complexes as well as their electrochemical properties. The molecular structure, absorption spectra, and photoelectric performance of DSSCs based on various metal complex [polypyridyl (Ru)] dyes are shown in Table 3 and Figure 12.

**TABLE 3 ABSORPTION SPECTRA AND PHOTOELECTRIC PERFORMANCE FOR DSSCS BASED ON DIFFERENT METAL COMPLEX**

| Dye            | Absorption coefficient $\epsilon$ ( $10^3 \text{ m}^2 \text{ mol}^{-1}$ ) | IPCE (%) | $J_{SC}$ ( $\text{mAcm}^{-2}$ ) | $V_{OC}$ (V) | FF    | $\eta$ (%) |
|----------------|---|----------|---------------------------------|--------------|-------|------------|
| N3             | 534   | 83       | 18.20                           | 720          | 0.730 | 10.00      |
| N719           | 532   | 85       | 17.73                           | 846          | 0.750 | 11.18      |
| N749 black dye | 605   | 80       | 20.53                           | 720          | 0.704 | 10.40      |
| N749           | -   | 80       | 20.90                           | 736          | 0.722 | 11.10      |
| Z907           | 526   | 72       | 13.60                           | 721          | 0.692 | 6.80       |
| Z907           | 526   | 72       | 14.60                           | 722          | 0.693 | 7.30       |
| K8             | 555   | 77       | 18.00                           | 640          | 0.750 | 8.64       |
| K19            | 543   | 70       | 14.61                           | 711          | 0.671 | 7.00       |
| N945           | 550   | 80       | 16.50                           | 790          | 0.720 | 9.60       |
| Z910           | 543   | 80       | 17.20                           | 777          | 0.764 | 10.20      |
| K73            | 545   | 80       | 17.22                           | 748          | 0.694 | 9.00       |
| K51            | 530   | 70       | 15.40                           | 738          | 0.685 | 7.80       |
| HRS-1          | 542   | 80       | 20.00                           | 680          | 0.690 | 9.50       |
| Z955           | 519   | 80       | 16.37                           | 707          | 0.693 | 8.00       |

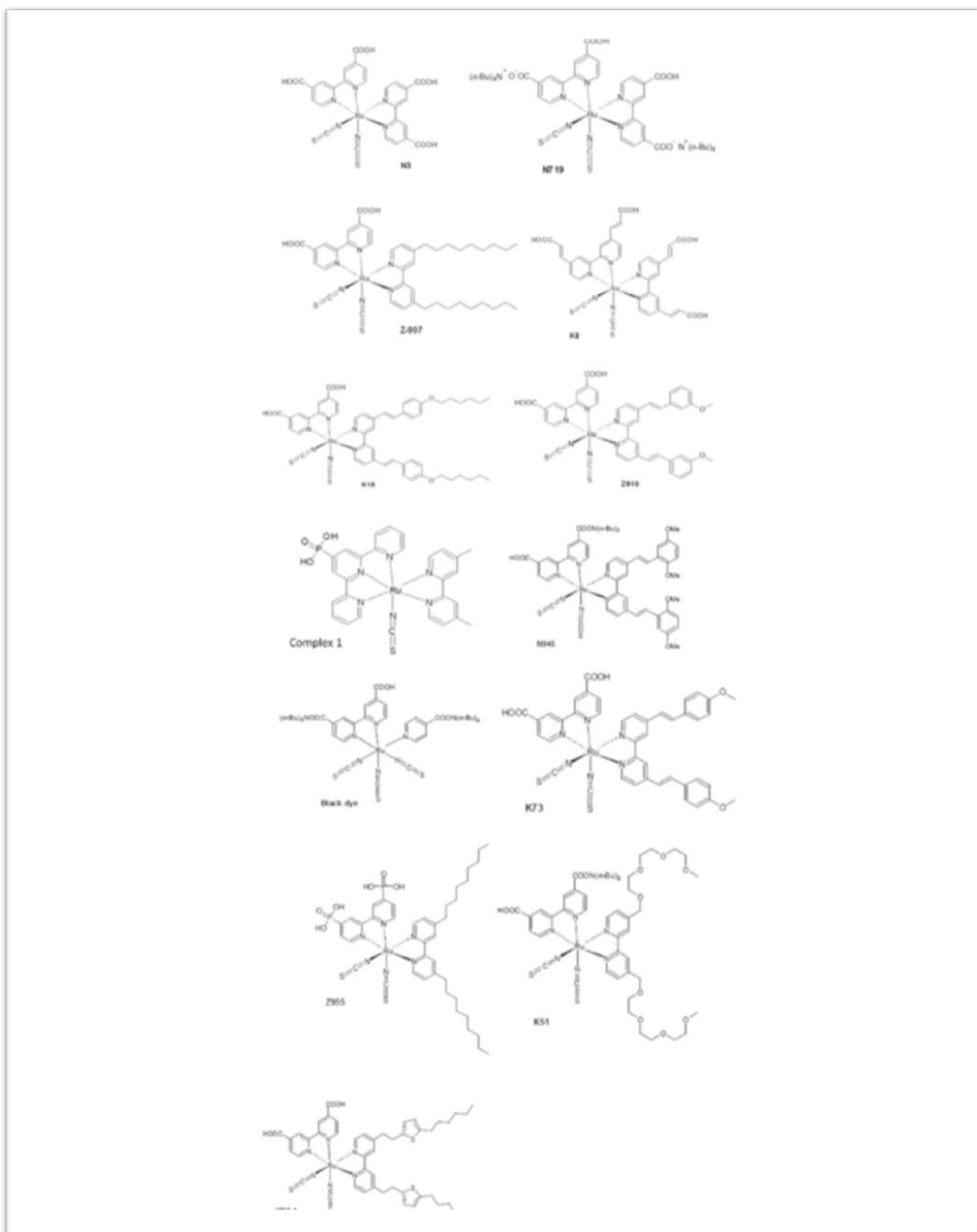


**FIG 10. MOLECULAR STRUCTURE OF RUTHENIUM COMPLEX BASED DYE SENSITIZERS**

### **N3/N719/N712 DYES**

Nazeeruddin et al. reported DSSC in 1993 using a Ruthenium (Ru)-complex dye called N3 dye cis-di(thiocyanato)bis(2,2-bipyridine-4,4-dicarboxylate)ruthenium, which contained one Ru centre and two thiocyanate ligands (LL') with additional carboxylate groups as anchoring sites and absorbed up to 800 nm radiations [26]. They achieved a 10.3% efficiency

with a system containing N3 dye and TBP treatment of the dye-covered film. This dye had maximum absorption spectra at 518 and 380 nm wavelengths, with extinction Since the start of the illumination, the dye has maintained a 60 ns excited state lifetime for more than 10 turnovers without significant decomposition [26]. Furthermore, by substituting ligands such as thiocyanate ligands and halogen ligands, the dye's absorption can be extended into the red and NIR. A device containing acetylacetonate, for example, demonstrated efficiency of = 6.0 percent [152], followed by a pteridinedione complex with 3.8 percent efficiency [88] and a diimine dithiolate complex with 3.7 percent efficiency [89]. coefficients of  $1.3 \times 10^4 \text{ M}^{-1} \text{ cm}^{-1}$  and  $1.33 \times 10^4 \text{ M}^{-1} \text{ cm}^{-1}$ , respectively.

## **II-SYSTEM EXTENSION (N945, Z910, K19, K73, K8, K9)**

Standard Ru complexes have a substantially lower absorption coefficient than other organic dyes, necessitating a thick layer of  $\text{TiO}_2$ , resulting in a larger electron recombination risk. Two carboxylic acid groups in N3 can thus be substituted by ligands containing conjugated  $\pi$ -systems to improve absorption and cell efficiency at the same time. The  $\pi$ -system extension in dyes is used to make sensitizers with greater molar extinction coefficients ( $\epsilon$ ), allowing the dye's LUMO to be tweaked for directionality in the excited state and the introduction of hydrophobic side chains that repel water and triiodide from the  $\text{TiO}_2$  surface. Rawashdeh et al. recently obtained a 0.45% efficiency by using a graphene-based transparent electrode sensitised with 0.2 mM N749 dye in ethanolic solution as the photoanode [90].

## **METAL-FREE, ORGANIC DYES**

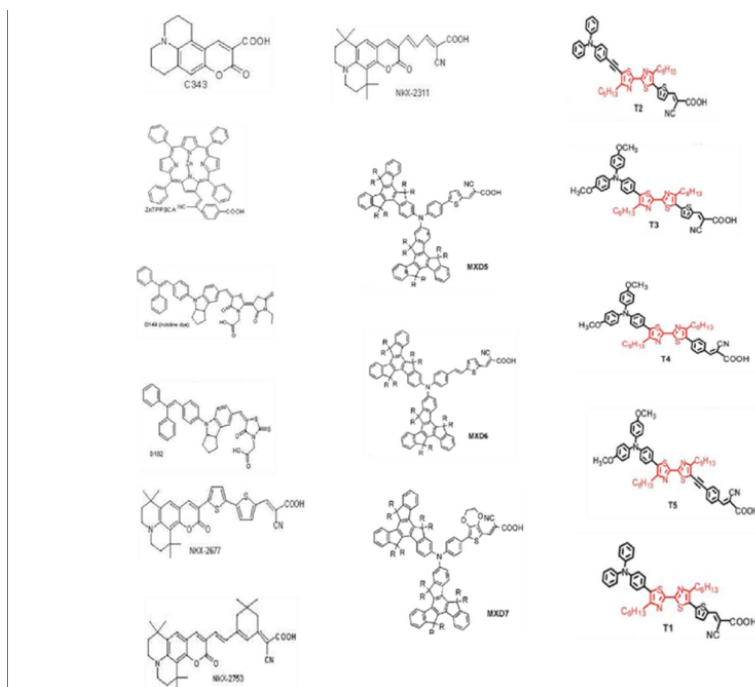
Despite their potential to produce highly efficient DSSCs, Ru dyes are only suited for DSSCs since Ru is a rare and expensive metal that is not suitable for cost-effective, environmentally friendly PV systems. As a result, new metal-free/organic dyes and natural colours must be developed and applied. The efficiency of DSSCs with organic dyes has grown dramatically in recent years, with Ito and colleagues reporting a 9 percent efficiency [91]. Table 4 and Fig. 16 exhibit the molecular structure and efficiency of DSSCs based on several metal-free organic dyes.

Table 4 The efficiency for DSSCs based on different metal-free organic dyes

| Dye      | Derivative      | Efficiency (%) |
|----------|-----------------|----------------|
| NKX-2311 | Coumarin        | 5.6            |
| NKX-2753 | Coumarin        | 6.7            |
| NKX-2677 | Coumarin        | 7.4            |
| D5       | TPA             | 5.1            |
| D149     | Indole          | 8              |
| DPI-T    | BPI             | 1.28           |
| D149     | Indole          | 9.0            |
| ZnTPPSCA | Porphyrin       | 4.2            |
| Zn2      | Porphyrin       | 4.8            |
| Zn3      | Porphyrin       | 5.6            |
| 2TPA-R   | TPA             | 2.3            |
| RD-Cou   | Coumarin        | 4.24           |
| IK3      | Indole          | 6.3            |
| LD4      | Zinc porphyrins | 10.06          |
| L2       | TPA             | 3.08           |
| MXD 7    | TPA             | 6.18           |
| Y123     | TPA             | 10.3           |
| T2-1     | PTZ             | 5.5            |
| PTZ-I    | PTZ             | 5.4            |
| S2       | Carbazole       | 6.02           |
| DPP-I    | DPP core        | 4.14           |

Thus, metal-free organic dyes are rapidly evolving to overcome the limits discussed above, with the fast learning curve holding particular promise for the future synthesis of novel materials with greater stability and, as a result, the design of highly efficient DSSCs at considerably lower costs. Though the efficiency of these dyes is less than that of Ru dyes, their applicability is broad since they are theoretically very cheap due to the integration of rare noble metals in organic dyes; hence, their cost is primarily determined by the number of synthesis steps involved. In comparison to Ru complexes, organic dyes have structure variations, low cost, a simple preparation process, and are environmentally friendly; additionally, the absorption coefficient of these organic dyes is typically one order of magnitude higher than Ru complexes,

allowing for the thin TiO<sub>2</sub> layer. As a result, there is a huge demand for new pure organic dyes to make DSSC commercialization easier.



**Fig 11** Molecular Structure of metal-free organic dyes

A good electron injection is one of the requirements for DSSCs, cyanoacetic acid and cyanoacrylic acid are commonly used as acceptor units because of their great electron withdrawing capacity. Yu et al included cyanoacrylic acid as a strong electron acceptor for D-n-A-based dyes because the dye incorporating cyanoacrylic acid as an electron acceptor produced the best results, and the DSSC achieved  $\eta=4.939$  percent [92] due to the maximum absorption spectrum and the highest molar excitation coefficient.

## COUMARIN DYES

Dyes Coumarin is a natural chemical present in many plants, including tonka bean, woodruff, and bison grass (molecular structure in Fig. 18a). Grätzel et al. discovered efficient electron injection rates of 200 fs from C343 into the TiO<sub>2</sub> conduction band in 1996, when transient investigations on a coumarin dye in DSSCs were undertaken for the first time [93]. However, the device's conversion efficiency was reduced due to C343's limited absorption spectrum, or lack of absorption in the visible range.[94] This can be changed by adding more methane groups, which results in the n-conjugation linkers enlarging and the DSSC [95 ] being more efficient. Giribabu and colleagues synthesised RD-Cou sensitizers with a conversion efficiency of 4.24 percent using liquid electrolyte, in which the coumarin moiety was bridged to the

pyridyl groups by thiophene, resulting in extended n-conjugation and broadening of the metal-to-ligand charge transfer spectra [96]. The absorption spectrum of RD-Cou dye was discovered to be centred at 498 nm with an  $\epsilon = 16,046 \text{ M}^{-1}\text{cm}^{-1}$ . Despite the lower efficiency of these cells, the dye showed thermal stability of up to 220 °C during thermal study, showing that they are viable.

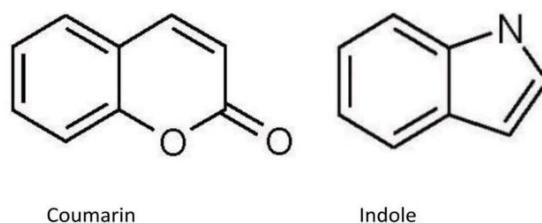


FIG 12 MOLECULAR STRUCTURE OF (A) COUMARIN AND (B) INDOLE

## INDOLE DYES

Indole is found naturally in the amino acid tryptophan, as well as several alkaloids and colours (molecular structure shown in above Fig. b). These dyes have shown good potential as a sensitizer when substituted with an electron withdrawing anchoring group on the benzene ring and an electron donating group on the nitrogen atom. As sensitizers, these dyes have shown to be effective. In general, an indole dye's D-A structure has an indole moiety acting as an electron donor and a rhodanine group acting as an electron acceptor. The absorbance in the infrared (IR) region of the visual spectra, as well as the absorption coefficient of the dye, can be greatly increased by inserting aromatic units into the core of the indoline structure [97]. With D102 dye, an efficiency of 6.19 percent was demonstrated, and by optimising the substituents, an efficiency of 8% was achieved with D149 dye [98]. Another dye, "D205," was created by regulating the aggregation of dye molecules, as an indoline dye with an n-octyl substituent on the rhodasubstitution improved the  $V_{oc}$  without revealing too much CDCA. However, the CDCA increased the  $V_{oc}$  of D205 by roughly 0.054 V, but had minimal effect on D149[99], which only increased by 0.006 V. However, combining CDCA and the n-octyl chain (D205) enhanced the  $V_{oc}$  by up to 0.710 V, which was 0.066 V higher (by 10.2%) than D149 with CDCA.

Wu et al. demonstrated  $\eta = 9.4$  percent in 2012, with  $J_{sc} = 18 \text{ mAcm}^{-2}$ ,  $V_{oc} = 0.69 \text{ V}$ , and  $FF = 0.78$ , by using indoline as an organic dye in the respective DSSC [100]. Suzuka et al. created a DSSC sensitised with indoline dyes in a quasi-solid gel form of the electrolyte, using highly reactive but resistant nitroxide radical molecules as redox mediator. At 1sun, they had an appreciable efficacy of 10.1 percent. They used lengthy alkyl chains that interact particularly with the radical mediator to represent a charge-recombination process at the dye contact [101]. Irgashev et al. recently synthesised a novel push-pull thieno[2,3-b]indole-based metal-free dye and explored its use in DSSCs [230]. They created IK 3-6 dyes based on the thieno[2,3-b]indole ring system with several aliphatic substituents, including the nitrogen atom as an electron-donating component, multiple thiophene units as a  $\pi$ -bridge linker, and 2-cyanoacrylic acid as an electron-accepting and anchoring group. Under simulated AM 1.5 G irradiation (100 mWcm), the DSSCs using 2-cyano-3-(15-[8-(2-ethylhexyl)-8H-thieno[2,3-b]indol-2-yl]thiophen-2-yl)acrylic acid (IK 3) had a 6.3 percent efficiency, but the dyes IK 5 and IK 6 had lower values of  $\eta = 1.3$  percent and 1.4 percent. The LUMO energy levels of all four dyes are more negative than the  $\text{TiO}_2$  conduction edge (-3.9 eV), and their HOMO energy levels are more positive than the  $\text{I}^-/\text{I}_3^-$  redox couple (-4.9 eV), allowing regeneration of oxidised dye molecules after injection of excited electrons into  $\text{TiO}_2$  electrode (as shown in Figure 19) [102]. The intermolecular  $\pi$ -stacking and aggregation activities on the photoanode surface contributed to the lower efficiency of other dyes.

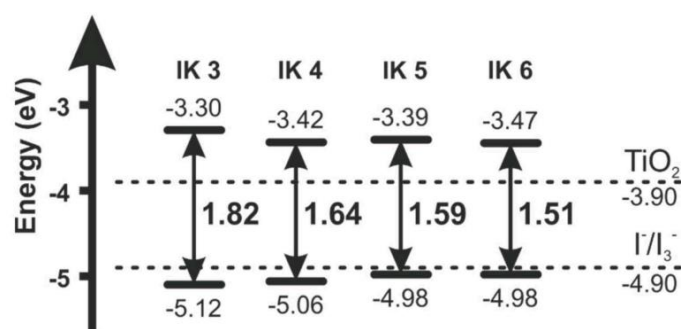


Fig 13 HOMO and LUMO energy level diagram of dyes IK 3-6

## TRIARYLAMINE DYES

The triarylamine group is frequently used as an HTM in various electronic devices because to its high electron and transporting capabilities, as well as its unique propeller starburst molecular structure with a nonplanar orientation.

Triarylamine derivatives distribute T-T stacking, improving cell performance by lowering charge recombination, eliminating dye aggregation, and increasing the organic dye's molar extinction coefficient [103,104,105]. The structural alteration of triarylamine derivatives could be accomplished by adding alkyl chains or donating groups [106,107,108]. By easily binding donor replacements on the n-linker of the dye [109], the performance of a basic D- $\pi$ -A organic dye can be improved. As a result, Prachumrak and colleagues have developed three new molecularly designed D- $\pi$ -A dyes, notably T2-4, which consists of TPA as a donor, terthiophene with various numbers of TPA substitutions as an n-conjugated linker, and cyanoacrylic acid as an acceptor [109]. To reduce electron recombination between the redox electrolyte and the TiO<sub>2</sub> surface while also increasing electron correction efficiency, electron donating TPA replacements on the n-linker of the D-T-A dye can play a beneficial role, leading to increased V<sub>oc</sub> and J<sub>sc</sub> [110].

In 2006, Hagberg et al. released a report on TPA-based D5 dye [110], demonstrating that the overall PCE for D5 dye was 5.1 percent, compared to 6.40 percent for standard N719 dye under similar manufacturing conditions. As a result, D5 arose as a foundation structure for the next series of TPA derivatives. By systematically increasing the conjugation of TPA-based organic dyes, a series L0-L4 was disclosed in 2007[111]. The molar extinction coefficients and absorption spectra of L0-L4 were improved by increasing the n conjugation. The observed IPCE spectra for L0 and L1 dyes were high, but the spectra of these dyes were not broad; as a result, lower conversion efficiencies were obtained for L0 and L1, whereas the broad absorption spectrum as well as the broad IPCE was obtained for L3 and L4 by augmentation of linker conjugation, but the efficiencies observed were less than for L0 and L1 due to the amount of dye loading, i.e., with an increase in the size As a result, the decreased IPCE for longer L3 and L4 could be attributed to poor TiO<sub>2</sub> surface binding. Solar cells based on L1 and L2, with efficiencies of 2.75 and 3.08 percent, respectively, achieved higher efficiencies. Baheti et al. [112] made DSSCs using nanocrystalline anatase TiO and simple triarylamine-based dyes with fluorene and biphenyl linkers. They found that the fluorene-based dyes outperformed the biphenyl counterparts in solar cell characteristics.

Lu et al. published a paper in 2011 detailing the synthesis, photo physical /electrochemical characteristics, and application of three functional triarylamine organic dyes (MXD5-7) in dye-sensitized solar cells. They employed the nonplanar structures of bishexapropyltruxeneamino as an electron donor [113] and looked at the effect of adding chenodeoxycholic acid (CDCA) to the dyes, finding that MXD5-7 without CDCA had lower photo current and efficiency than MXD5-7 with 3 mM CDCA. Under conventional global AM 1.5 sun conditions, the best efficiency of 6.18 percent was observed for MXD7 (with 3 mM CDCA) with electron lifetime ( $\tau$ ) = 63 ms (molecular structure shown in Table 4).

### **PHENOTHIAZINE (PTZ) DYES**

Phenothiazine is a heterocyclic molecule with electron-rich sulphur and nitrogen heteroatoms that has a non-planar and butterfly shape in the ground state, which can prevent molecular aggregation and the production of intermolecular excimers. As a result, PTZ emerges as a promising hole transport semiconductor in organic devices, with distinct electrical and optical features [114].

Tian and work mates investigated the effect of PTZ as an electron-donating unit in DSSCs, and they discovered that sensitizers based on PTZ performed better than those based on TPA [115] because PTZ has a stronger electron-donating tendency than TPA (0.848 and 1.04 V vs. the normal hydrogen electrode (NHE) [116]. T2-1 to T2-4, a new family of PTZ-based dyes, were demonstrated in 2007 [251]. The PTZ unit served as an electron donor in these dyes, while cyanoacrylic acid or rhodanine-3-acetic acid served as an electron acceptor, and alkyl chains were employed to boost solubility.

### **CARBAZOLE DYES**

It's a non-planar chemical that can boost materials' hole carrying ability while also preventing dye aggregation development [117]. This molecule has been used as an active component in solar cells due to its unique optical, electrical, and chemical properties [118,119].

The thermal stability and glassy state durability of organic molecules were greatly increased with the addition of the carbazole unit to the structure [120,121]. Tian et al. reported a 6.02 percent efficiency for DSSCs using S4 dye as a sensitizer and an additional carbazole moiety to the outside of the

donor group, and discovered that the additional moiety facilitated charge separation, lowering the recombination rate between conduction band electrons and the oxidized sensitizer [122].

Koumura et al. reported a series of MK-1, MK-2, and MK-3 dyes based on carbazole, where MK-1 and MK-2 have alkyl groups while MK-3 does not. They found that the presence of alkyl groups increased electron lifespan and therefore  $v_{oc}$  in mk-1 and mk-2 [123,124,125], and that the absence of alkyl groups could be responsible for the recombination process between conduction band electrons and dye cations in MK-3. New structural dyes, such as DA- $\pi$ -A type and D-D- $\pi$ -A-type organic dyes, have been produced by adding a subordinate donor-acceptor such as 3,6-ditert-butylcarbazole-2,3-diphenylquinoxaline to ease electron movement, reduce dye aggregation, and improve photostability [126].

## NATURAL DYES

Due to the intrinsic features of Ru(II)-based dyes, new dye materials are also being researched extensively, and in order to replace these uncommon and expensive Ru(I) complexes, natural dyes are being used as an alternative [127].

Natural colours are inexpensive and safe for the environment. Anthocyanin [127], chlorophyll [128], flavonoid [129], carotenoid [130], and other natural colours have been utilised as sensitizers in DSSCs. The availability and colour ranges of these dyes are listed in Table 5.

| Sensitizer  | Availability   | Color range   |
|-------------|--|---|
| Anthocyanin | Flowers, fruits, leaves, roots, tubers, and stems of the plant   | Purple red  |
| Carotenoid  | Fruits, flowers of plants, and microorganisms                    | (a) Red, yellow, and orange colors to flowers and fruits<br>(b) Yellow to orange petal colors |
| Chlorophyll | Leaves of mostly green plants, algae, and cyanobacteria          | Green   |
| Flavonoid   | Plants including angiosperms, gymnosperms, ferns, and bryophytes | Various colors of flavonoids are determined by the degree of oxidation of the C-ring          |

**TABLE 5 AVAILABILITY AND COLOUR RANGE FOR THE NATURAL DYES (ANTHOCYANIN, CAROTENOID, CHLOROPHYLL, AND FLAVONOID)**

## MOLECULAR STRUCTURE

### ➤ Anthocyanin; Figure 14

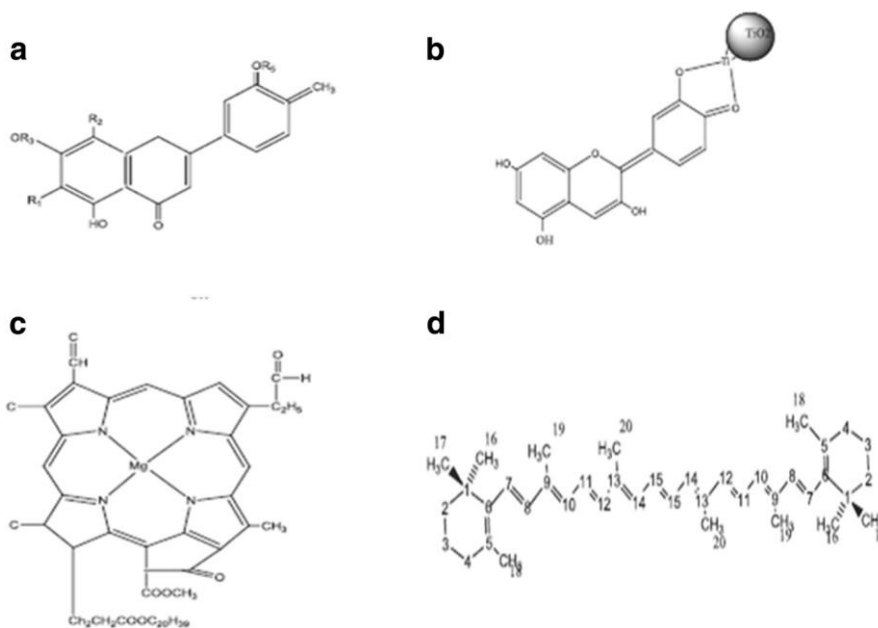
a depicts the molecular structure of anthocyanin. The carbonyl and hydroxyl groups of anthocyanin molecules are attached to the semiconductor ( $TiO_2$ )

surface, stimulating electron transfer from the sensitizer (anthocyanin molecules) to the conduction band of porous semiconducting ( $\text{TiO}_2$ ) film. Anthocyanin absorbs light and transfers it to the anthocyanin pair in the photosystem's reaction center via resonance energy transfers [131].

Flavonoid; As illustrated in Fig. 14b [132], flavonoid is a vast collection of natural dyes with a carbon framework (C<sub>6</sub>-C<sub>3</sub>- Co) or, more specifically, the phenylbenzopyran activity. It has 15 carbon atoms, with two phenyl rings joined by three carbon bridges to form a third ring, the colour of which is determined by the degree of phenyl ring oxidation (C-ring). It quickly adsorbs to a mesoporous  $\text{TiO}_2$  surface by displacing an OH counter ion from Ti sites, which then combines with a proton provided by the flavonoid [133].

Carotenoids; Andanthocyanin, flavonoids, and carotenoids are frequently found together in the same organs [134]. Carotenoids are naturally occurring chemicals that contain eight isoprenoid units (as shown in Fig. 14c). In dark and bright settings, beta-carotene dye has the highest photoconductivity of  $8.2 \times 10^{-4}$  and  $28.3 \times 10^{-4}$  (Q.m), respectively, [135] and has tremendous potential as energy harvesters and sensitizers for DSSCs [136].

Chlorophyll; Chl  $\alpha$  is the most common kind of chlorophyll pigment among the six that exist. Depending on the Chl type, it has a chlorine ring with a Mg centre, as well as varied side chains and a hydrocarbon trail.



CHEMICAL STRUCTURES OF A) ANTHOCYANIN, B) FLAVONOID, C) B.8-CAROTENE, AND D) CHLOROPHYLL

## ORGANIC COMPLEXES OF OTHER METALS

Other materials that could be used in DSSCs include Os, Fe, and Pt complexes [137,138,139]. Apart from being highly poisonous, Os complexes are used as a sensitizer in DSSCs due to their high absorption ( $\alpha_{811\text{nm}} = 1.5 \times 10^3 \text{ M}^{-1} \text{ cm}^{-1}$ ) and the use of spin prohibited singlet-triplet MLCT transition in the NIR. In this spectral region, higher IPCE values were obtained, but the overall conversion efficiency was only 50% of that of a normal Ru dye. The solvatochromism of complexes like  $[\text{Fe}(\text{L})_2(\text{CN})_2]$  can be used to adjust their ground and excited state potentials and increase the driving force for electron injection into the semiconductor conduction band or for regeneration of the oxidised dye by the electrolyte couple [139], which is very interesting due to the vast abundance of the metal and its non-toxicity.

## **LATEST APPROACHES AND TREND**

However, a new trend has emerged to improve the performance of DSSCs by including energy-introducing electrolyte relay dyes (ERDs) [57, 140]; chromophores with phosphorescence or luminescence, such as using rare-earth doped oxides in the DSSC [58-60]; and applying a luminous layer to the window glass [50,51] Photoanode The ERDs are being added now. Some highly luminous fluorophores must be added to the electrolyte or the HTM. The fluorescence (Forster) resonance energy transfer (FRET) [141] phenomenon is used by ERD molecules in DSSCs to absorb light that is not in the primary absorption spectrum region of the synthesis dye and then transmit the energy non-radiatively to the sensitising dyes. Siegers and colleagues [142] observed a 5 to 10% increase in external quantum efficiency in the spectral region 400 to 500 nm. Lin et colleagues. recently reported doping of a 1,8-naphthalimide (N-Bu) derivative fluorophore directly into a  $\text{TiO}_2$  mesoporous filament with N719 for use in DSSCs [143], in which the N-Bu served as the FRET donor and transferred energy to the N719 molecules via spectral down-conversion (FRET acceptor). At 1 sun (AM 1.5) illumination, the cell improved the PCE from 7.63 to 8.13 percent. Prathiwi et al. created a DSSC in 2017 by mixing a synthetic dye with a natural dye containing anthocyanin (from red cabbage) [144]. They made anthocyanin dye in a 10 ml volume and combination dyes in an 8 ml (anthocyanin): 2 ml (N719 synthetic dye) volume. They observed a 125 percent increase in conversion efficiency since the solo anthocyanin dye had a conversion efficiency of 0.024 percent, but the combination dye had a conversion efficiency of 0.054 percent.

Because of the higher light absorption, this augmentation was considered. As a result, more photons were absorbed, and the number of electrons in the excited state grew, boosting the photocurrent. Thus, cocktail dyes are becoming a new fad in DSSCs. When chlorophyll dye (from wormwood) and anthocyanin dye (from purple cabbage) as natural dyes were mixed together at a volume ratio of 1:1, Chang et al. achieved a  $\eta = 147$  percent conversion efficiency [145], although the individual dyes had lower conversion efficiencies. Puspitasari et al. created various DSSCs by combining three natural dyes: The mixture of the three dyes had the maximum efficiency of 0.0566 percent, with the absorbance peak of the mixed dyes being detected at 300 nm and 432 nm [106]. When mixing the chlorophyll and xanthophyll dyes together, Lim and colleagues produced a 0.085 percent efficiency [146]. In 2018, Konno et al. investigated the PV properties of DSSCs by mixing different dyes and found that the combination dye "D358 + D131" had the greatest  $\eta = 3.03$  percent [147]. Figure 24 depicts the IPCE of single and blended pigments: urmeric, mangosteen, and chlorophyll.

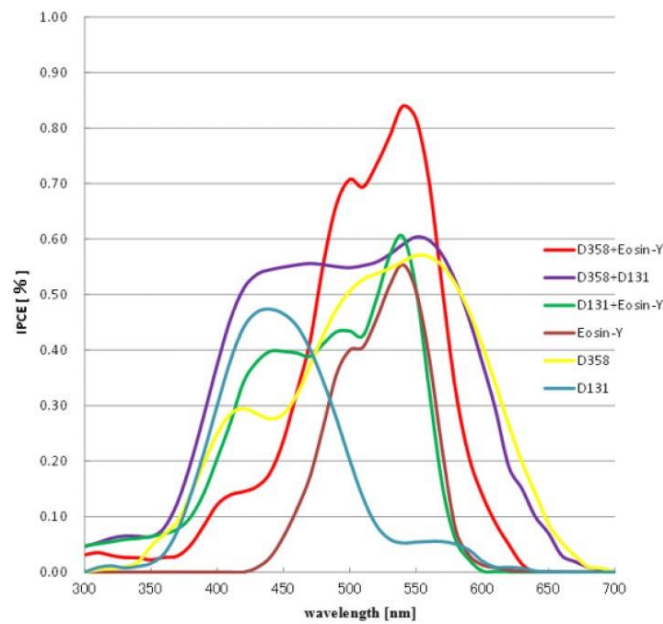


FIG 15 IPCE OF MIXED PIGMENT AND SINGLE PIGMENTS, WHERE SINGLE PIGMENT WERE EOSIN Y, D131, AND D358 AND MIXED PIGMENTS WERE D358 AND EOSIN Y; D358 AND D131; D131 AND EOSIN Y [311]

## APPROACH

The plasmonic effect is one method of improving the performance of DSSCs. SPR is a resonant oscillation of conduction electrons at the border between negative and positive permittivity materials that is stimulated by incoming

light. Gangishetty and colleagues created core-shell NPs in 2013 that included a triangular nanoprism core and a variable-thickness silica shell. For the nanoprism Ag particles, an SPR band centred at 730 nm was discovered, which closely overlapped the N719 absorption spectrum's edge. They discovered that adding nanoprism Ag particles to the photoanode of DSSCs increased the overall PCE by 32% [148]. Hossain et al. investigated the effect of SiO<sub>2</sub>-encapsulated Ag nanoparticles in DSSCs using the plasmonic phenomena with varying numbers of silver nanoparticles (Ag NPs) coated with a SiO<sub>2</sub> layer pre prepped as core shell Ag@SiO<sub>2</sub> [Silver and silicacoatedsilvernanoarticles] (Ag@SiO<sub>2</sub> nanoparticles (Ag@SiO NPs). They discovered that a photoanode incorporating 3 wt percent Ag@SiO had the highest PCE of 6.16 percent, which was 43.25 percent greater than a 0 wt percent Ag@SiO, NP photoanode [149]. However, for 4 wt percent Ag@SiO<sub>2</sub> and 5 wt percent Ag@SiO, a simultaneous decrease in efficiency with additional increases in the wt percent ratio was seen. The decrease in excess quantities of Ag@SiO<sub>2</sub> NPs was related to three factors: (i) a reduction in the films' effective surface area, I less dye absorption, and (ii) an increase in charge-carrier recombination [150]. Following an examination of the nyquist plots (as shown in Fig. 25), They discovered that when the Ag@SiO, NP content climbed to 3 wt%, the diameter of Z<sub>2</sub> reduced monotonically, and R<sub>2</sub> decreased from 10.4 to 6.64 Q for the normal DSSC to the 3 wt% Ag@iO<sub>2</sub> NPs containing DSSC. Jun et al. created plasmonic effects in DSSCs using quantum-sized gold NPs (151).

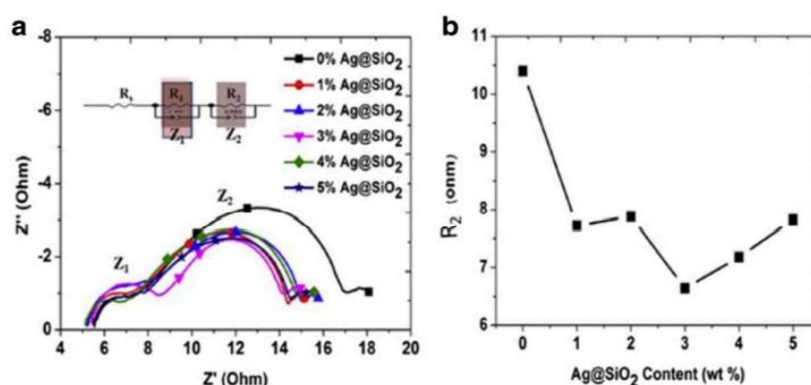


Fig 16 Nyquist plots obtained from the EIS of DSSCs with varying Ag@SiO<sub>2</sub> content (inset shows the equivalent circuit). B) R<sub>2</sub> ohm with respect to the Ag@SiO<sub>2</sub> NPs content [313]

## CONCLUSION

The main goal of this research was to conduct a complete analysis of new materials for photoanodes, counter sensitizers, electrodes and electrolytes , in order to develop DSSCs that are low-cost, flexible, environmentally sustainable, and simple to make. Even so, a brief explanation has been provided to better understand the working and composition of this article, which aims to establish a link between the photosensitizer structure, interfacial charge transfer reactions, and device performance, all of which are important to understand when developing new metal and metal-free organic dyes. In order to address the low stability provided by DSSCs, this work focused on two primary issues: low intrinsic stability and electrolyte sealing. We have two best conceivable alternatives for meeting the massive demand for electricity and power: nuclear fission or the sun. Even said, nuclear fission, which is anticipated to be the greatest option, has significant environmental concerns as well as waste management issues. As a result, the second option is preferable. DSSCs were created as a low-cost alternative, however their efficiency in the field is insufficient. As a result, we must conduct extensive research into all areas of DSSCs. New photosensitizers based on metal complexes of Ru or Os organic metal-free complexes/natural dyes; and new electrolytes based on imidazolium salts/pyridinium salts/conjugated polymers, gel electrolytes, polymer electrolytes, and water-based electrolytes were presented.

In conclusion, extensive studies have been conducted to address individual challenges associated with working electrodes, dyes, and electrolytes separately; thus, a comprehensive approach is required to address all of these issues by selecting appropriate electrolyte conditions (both in

terms of material and structure), optimum dye, and the most stable electrolyte that provides better electron transportation capability. In terms of commercial applications, a DSSC must last for more than 25 years in building-integrated modules to avoid causing disruption to the building environment during repair or replacement, and a lifespan of 5 years is sufficient for portable electronic chargers integrated into apparel and accessories [152]. However, because of their sandwiched glass construction, DSSCs are extremely bulky; however, flexible DSSCs (described elsewhere) that may be processed using roll-to-roll technologies may be a viable alternative, though they must accept a reduced lifespan. Although, as previously said, the encapsulation and sealing of a DSSC are more likely to determine its stability and lifespan. Aside from the use of expensive glass substrates in the case of modules and panels, one of the most difficult challenges is producing glass that is flat at the 10  $\mu\text{m}$  length scale over regions much greater than 30 x 30 cm [153] and humidity. Another problem is determining which metal interconnects in the cells are more or less corroded by the electrolyte, as well as maintaining a high level of cell-to-cell reproducibility to produce the same current and/or voltage for all of the cells in the module. If the above problems are overcome, the commercial applications of DSSCs, which have been limited to an amicable extent, will no longer be a bottleneck. In 2007, G24i launched a 25 MW DSC module production line in Cardiff, Wales (UK), with ambitions to expand to 200 MW by the end of 2008, and numerous DSSC demonstration modules are now available. However, the maximum Outdoor aging test of DSSCs is reported for 2.5 years up to now [154].

## REFERENCES

1. Tributsch H, Calvin M (1971) Electrochemistry Of Excited Molecules: PhotoElectrochemical Reactions Of Chlorophylls. *Photochem Photobiol* 14:95-112.
2. Tsubomura H, Matsumura M, Nomura Y, Amamiya T (1976) Dye sensitised zinc oxide: aqueous electrolyte: platinum photocell. *Nature* 261:402-403.
3. O'Regan B, Gratzel M (1991) A low-cost, high-efficiency solar cell based on dye-sensitized colloidal TiO<sub>2</sub> films. *Nature* 353:737-740
4. Nazeeruddin K, Baranoff E, Gratzel M (2011) Dye-sensitized solar cells: A brief overview. *Energy* 36:1172-1178.
5. Altobello S, Bignozzi C (2004) A, Caramori S, Larramona G, Quici S, Marzanni G, Lakhmiri R; Sensitization of TiO<sub>2</sub> with ruthenium complexes containing boronic acid functions. *J Photochem Photobiol A Chem* 166:91-98.
6. Kunzmann A, Valero SE, Sepúlveda A, Rico-Santacruz M, Lalinde ER, Berenguer J, García-Matinez JM, Guldi D, Serrano ED, Costa R (2018) Hybrid Dye-Titania Nanoparticles for Superior Low-Temperature Dye-Sensitized Solar Cells. *Adv Energy Mat* 8:121-212.
7. Snaith HJ (2010) Estimating the Maximum Attainable Efficiency in Dye sensitized Solar Cells. *Adv Funct Mater* 20:13-19.
8. Frank A, Kopidakis N, De Lagemaat Jv (2004) Electrons in nanostructured TiO<sub>2</sub> solar cells: Transport, recombination and photovoltaic properties. *Coord Chem Rev* 248:1165-1179.
9. Anandan S (2007) Recent improvements and arising challenges in dye-sensitized solar cells. *Sol Energy Mater Sol Cells* 91:843-846.
10. Anandan S, Madhavan J, Maruthamuthu P, Raghukumar V, Ramakrishnan VI (2004) Synthesis and characterization of naphthyridine and acridinedione ligands coordinated ruthenium (II) complexes and their applications in dye sensitized solar cells. *Sol Energy Mater Sol Cells* 81:419-428.
11. Bose S, Soni Vand Genwa KR (2015) Recent Advances and Future Prospects for Dye Sensitized solar Cells: A Review. *Int J Sci Res Pubs* 4.
12. Web reference available online at <http://www.sta.com.au/downloads/DSC9%20Booklet.pdf>

13. Shalini S, Balasundaraprabhu R, Satish Kumar T, Prabavathy N, Senthilarasu S, Prasanna S (2016) Status and outlook of sensitizers/dyes used in dye sensitized solar cells (DSSC: a review: Sensitizers for DSSC. *Int J Energy Res* 0:1303-1320.
14. . Wu J, Lan Z, Lin J, Huang M, Huang Y, Fan L, Luo G, Lin Y, Xie Y, Wei Y 201/) Counter electrodes in dye-sensitized solar cells. *Chem SoC Hev* 46 5975-6023.
15. Kakiage K, Aoyama Y, Yano T, Oya K, Fujisawab J, Hanaya M (2015) Highlyefficient dye-sensitized solar cells with collaborative sensitization by silyanchor and carboxy-anchor dyes. *Chem Commun* 51:15894-15897.
16. Yeoh ME, Chan KY (201/) Recent advances in photo-anode for dye sensitized solar cells: a review. *IntJ Energy Res* 41:2446-2467.
17. Fan K Yu J, Ho W (2017) Improving photoanodes to obtain highly efficient dye-sensitized solar cells: a brief review. *Mater Horiz* 4:319-344.
18. 18. Mehmood U (2014) Rahman S, Harrabi K, Hussein IA, Reddy BVS, Recent advances in dye sensitized solar cells. *Advances in Materials Science and Engineering Article ID* 974782:1-12.
19. Andualem A, Demiss S (2018) Review on Dye-Sensitized Solar Cells (DSSCS) *Edelweiss Appli Sci Tech* 2:145-150.
20. Grant FA (1959) Properties of Rutile (Titanium Dioxide). *Rev Mod Phys* 31: 646-674.
21. Bickley RI (1978) *Chem Phys Solids Surf* 7:118
22. Tennakone K, Kumara GRRA, Kottegoda IRM, VPS P (1999) An efficient dyesensitized photoelectrochemical solar cell made from oxides of tin and zinc *Chem Comm* 1:15-16
23. Sayama K, Sugihara H, Arakawa H (1 998) Photoelectrochemical Properties of Porous NbO<sub>5</sub> Electrode Sensitized by a Ruthenium Dye. *Chem Mater* 10: 3825
24. Fung AKM, Chiu B (2003) K W, Lam M H W; Surface modification of TiO<sub>2</sub> by a ruthenium() polypyridyl complex via silyl linkage for the sensitized photocatalytic degradation of carbon tetrachloride by visible irradiation. *Water Res* 37:1939-1947.
25. Zaban A, Ferrere S, Gregg BA (1998) Relative Energetics at the Semiconductor/ ensitizing LDye/Electrolyte Interface. *J Phys Chem* 102:452-460.
26. Nazeeruddin MK, Kay A, Rodicio I, Humphry-Baker R, Mueller E, Liska P, Viachopoulos N, Graetzel M (1993) Conversion of light to electricity by ci X<sub>2</sub>bis(2,2-bipyridyl-4,4-dicarboxylate)ruthenium(III) charge-transfer sensitizers on nanocrystalline titanium dioxide electrodes. *J Am Chem Soc* 115:6382-6390.
27. Hagberg DP, Yum JH, Lee H, De Angelis F, Marinado T, Karlsson KM, Humphry-Baker R, Sun L, Hagfeldt A, Grätzel M, Nazeeruddin MK (2008) Molecular engineering of organic sensitizers for dye-sensitized solar cell applications. *J Am Chem Soc* 130:6259-6266.
28. Neale NR, Kopidakis N, van de Lagemaat J, Grätzel M, Frank AJ (2005) Effect of a Coadsorbent on the Performance of Dye-Sensitized TiO<sub>2</sub> Solar Cells: Shielding versus Band-Edge Movement. *J PhysChem B* 109:23183-23189.
29. errere s, Laban A, GreggBA (199/) Dye Sensitization of Nanocrystalline lin Oxide by Penylene Derivatives. *J Phys Chem B* 101:4490-4493.

30. Oskam G, Bergeron BV, Meyer GJ, Searson PC (2001) Pseudohalogens for Dye sensitized TiO<sub>2</sub> photoelectrochemical cell. *J Phys Chem B* 105:6867-6873
31. Nusbaumer H, Moser JE (2001) Zakeeruddin SM et al; Co<sup>II</sup>(dbbip)<sup>-</sup> complex rivals triiodide/iodide redox mediator in dye sensitized photovoltaic cells. *J Phys Chem B* 105:10461-10464.
32. Gao F, Wang Y, Shi D, Zhang J, Wang M, Jing X, Humphry-Baker R, Wang P, Zakeeruddin SM, Grätzel M (2008) Enhance the optical absorptivity of nanocrystalline TiO<sub>2</sub> film with high molar extinction coefficient ruthenium sensitizers for high performance dye sensitized solar cells. *J Am Chem Soc* 130(32):10720-10728.
33. Wu J, Lan Z, Hao S, Li P, Lin J (2008) Huang M et al; Progress on the electrolytes for Dye-sensitized solar cells. *Pure Appl Chem* 80:2241-2258.
34. Toivola M, Ahlskog , Lund P (2005) Industrial sheet metals for nanocrystalline dye-sensitized solar cell structures. *Sol Energy Mater Sol Cells* 90:2881-2893.
35. Kay HA, Grätzel M (1996) Low cost photovoltaic modules based on dye sensitized nanocrystalline titanium dioxide and carbon powder. *Sol Energy Mater Sol Cells* 44:99-117.
36. Wang M, Anghel AM, Marsan B, Cevey Ha NL, Pootrakulchote N, Zakeeruddin SM, Grätzel M (2009) Co<sup>II</sup> Supersedes Pt as Efficient Electrocatalyst for Triiodide Reduction in Dye-Sensitized Solar Cells. *J Am Chem Soc* 131:15976-15977.
37. Fakharuddin A, Jose R, Brown TM, Fabregat-Santiago F, Bisquert J (2014) A perspective on the production of dye-sensitized solar modules. *Energy Environ Sci* 7:3952-3981.
38. Grätzel M and Moser JE; *Solar Energy Conversion, Electron Transfer in chemistry* (Ed: V. Balzani) *Energy and the environment* (Ed: I. Gould) (2001) 5:589-644.
39. Wang H-J, Chen CP, Jeng RJ (2014) Polythiophenes Comprising Conjugated Pendant for Polymer Solar Cells: A Review. *Materials* 7(4):2411-2439.
40. Grätzel M (2005) *Solar Energy Conversion by Dye-Sensitized Photovoltaic Cells*. *Inorg Chem* 44:6841-6851.
41. Cai H, Tanga Q, He B, Lia R, Yu L (2014) Bifacial dye-sensitized solar cells with enhanced rear efficiency and power output. *Nanoscale* 6:15127-15133.
42. Liu J, Tang Q, He B, Yu L (2015) Cost-effective, transparent iron selenide nanoporous alloy counter electrode for bifacial dye-sensitized solar cell. *J Mater Sci* 282:79-86.
43. Kusama H, Orita H, Sugihara H (2008) TiO<sub>2</sub> Band Shift by Nitrogen-Containing Heterocycles in Dye-Sensitized Solar Cells: a Periodic Density Functional Theory Study. *Langmuir* 24:4411-4419
44. Murakami TN, Grätzel M (2008) Counter electrode for DSC: application of functional materials as catalysts. *Inorg Chim Acta* 361:572-580
45. Murakami Iha NY, Garcia CG, Bignozzi CA (2003) Dye-sensitized photoelectrochemical cells. In: Nalwa HS (ed) *Handbook of photochemistry and photobiology*. American Scientific Publishers, Stevenson Ranch, California, USA, pp49-82
46. Hardin BE, Hoke ET, Armstrong PB, Yum JH, Comte P et al (2009) Increased light harvesting in dye-sensitized solar cells with energy relay dyes. *Nat Photonics* 3:406-411.

47. Wang J, Wu J, Lin J, Huang M, Huang Y et al (2012) Application of Y<sup>3+</sup>, Er<sup>3+</sup> Nanorods in Dye-Sensitized Solar Cells. *Chem Sus Chem* 5:1307-1312.
48. Li L, Yang Y, Fan R, Jiang Y et al (2014) A simple modification of near infrared photon-to-electron response with fluorescence resonance energy transfer for dye-sensitized solar cells. *J Power Sources* 264:254-261
49. Chander N, Khanb AF, Komarala VK (2015) Improved stability and enhanced efficiency of dye sensitized solar cells by using europium doped yttrium vanadate down-shifting nanophosphor. *RSC Adv* 5:66057-66066
50. Wang TH, Huang 1W, Tsai YC, Chang YVW, Liao CS (2015) A photoluminescent layer for improving the performance of dye-sensitized solar cells. *Chem Commun* 51:7253-7256
51. Han DM, Song HJ, Han CH, Kim YS (2015) Enhancement of the outdoor stability of dye-sensitized solar cells by a spectrum conversion layer with 6-hapnthalimide derivatives. *RSC Adv* 5:32588-32593.
52. Bakr NA, Ali AK, Jassim SM (2017) Fabrication and Efficiency Enhancement of Z907 Dye Sensitized Solar Cell Using Gold Nanoparticles. *J Advan Phys* 63):370-374.
53. Wang P, Zakeeruddin SM, Baker RH, Moser JE, Gratzel M (2003) Molecular Scale interface engineering of TiO<sub>2</sub> nanocrystals: Improving the efficiency and stability of dye sensitized solar cells. *Adv Mater* 15:2101-2104.
54. Gao R, Cui Y, Liu X, Wang L (2014) Multifunctional Interface Modification of Energy Relay Dye in Quasi-solid Dye-sensitized Solar Cells. *Sci Rep* 4:5570
55. Rahman MM, Kob MU, Lee JJ (2015) Novel energy relay dyes for high efficiency dye-sensitized solar cells. *Nanoscale* 7:3526-3531.
56. Hagfeldt A, Gratzel M (1995) Light-Induced Redox Reactions in Nanocrystalline systems. *Chem Rev* 95:49-08.
57. Kalyanasundaram K, Gratzel M (1998) Applications of functionalized transition metal complexes in photonic and optoelectronic devices. *Coord Chem Rev* 177:347-414.
58. Aye MM, Win TT, Maung YM, Soe KKK (2014) Binary Oxide Photoelectrode with Coffee Natural Dye Extract for DSSC Application. *Int J Innov Sci Res* 8(2):276-282.
59. Lee KM, Hu CW, Chen HW, Ho KC (2008) Incorporating carbon nanotube in a low-temperature fabrication process for dye-sensitized TiO<sub>2</sub> solar cells. *Sol Energy Mater Sol Cells* 92:1628-1633.
60. Muduli S, Lee W, Dhas V, Mujawar S, Dubey M, Vijayamohanan K, Han SH, Ogale S (2009) Enhanced Conversion Efficiency in Dye-Sensitized Solar Cells Based on

Hydrothermally Synthesized TiO<sub>2</sub>-MWCNT Nanocomposites. *Appl Mater Interface* 1:2030-2035.

61. Lee W, Lee J, Min SK et al (2009) Effect of single-walled carbon nanotubes in PbS/TiO<sub>2</sub> quantum dots-sensitized solar cells. *Mater Sci Eng B* 156:48-51.
62. Sun SR, Gao L, Liu YQ et al (2010) Enhanced dye-sensitized solar cells using graphene-TiO<sub>2</sub> photoanode prepared by heterogeneous coagulation. *Appl Phys Lett* 96:083113-083115.
63. Sharma GD, Daphnomili D, Gupta KSV, Gayathri T et al (2013) Enhancement of power conversion efficiency of dye-sensitized solar cells by co sensitization of zinc-porphyrin and thiocyanate-free ruthenium(II)-terpyridine dyes and graphene modified TiO<sub>2</sub> photoanode. *RSC Adv* 3:22412-22420.
64. Tathavadekar M, Biswal M, Agarkar S, Giribabu L, Ogale S (2014) Electronically and catalytically functional carbon cloth as a permeable and flexible counter electrode for dye sensitized solar cell. *Electrochim Acta* 123:2485.
65. Jiang OW, Lia GR, Gao XP; Highly ordered TiN nanotube arrays as counter electrodes for dye-sensitized solar cells (2009) *Chem Commun* 06/20-6722.
66. Li GR, Wang F, Jiang QW, Gao XP, Shen PW (2010) Carbon nanotubes with titanium nitride as a low-cost counter-electrode material for dye-sensitized solar cells. *Angew Chem Int Ed* 49:3653-3656.
67. Sun H, Zhanga L, Wang ZS (2014) Single-crystal CoSe<sub>2</sub> nanorods as an efficient electrocatalyst for dye-sensitized solar cells. *J Mater Chem A* 2: 16023-16029
68. Banerjee A, Upadhyay KK, Bhatnagar S, Tathavadekar M et al (2014) Nickel cobalt sulfide nanoneedle array as an effective alternative to Pt as a counter electrode in dye sensitized solar cells. *RSC Adv* 4:8289 -8294.
69. Maheswari D, Venkatachalam P (2015) Fabrication of High Efficiency Dye Sensitized Solar Cell with Zirconia-Doped TiO<sub>2</sub> Nanoparticle and Nanowire Composite Photoanode Film. *Aust J Chem* 68:881-888.
70. Swathi KE, Jinchu I, Sreelatha KS, Sreekala CO, Menon SK (2018) Effect of microwave exposure on the photo anode of DSSC sensitized with natural dye. *IOP Conf ser: Mater Sci Eng* 3100012141.
71. Guo M, Yao Y, Zhao F, Wang S, Xiao J (2017) An In<sub>2</sub>S<sub>3</sub>@Conductive carbon composite with superior electrocatalytic activity for dye-sensitized solar cells, *J. Photochem. Photobiol. A*. 332:8/-91
72. Tsi CH, Huang WC, Hsu YC, Shih CJ, Tenj IJ, YU YH (2016) Poly(omethoxyaniline) doped with an organic acid as low-cost-efficient counter electrodes for dye-sensitized solar cells. *Electrochim Acta* 213:791-801.

73. Liu I, Hou YC, Lia CW, Lee YL (2017) Highly electrocatalytic counter electrodes based on carbon black for cobalt(II)/VO-mediated dye-sensitized solar cells. *J Mater Chem A* 5:240-249.
74. Tsai CH, Fei PH, Chen CH (2015) Investigation of Coral-Like Cu<sub>2</sub>O Nano/Microstructures as Counter Electrodes for Dye-Sensitized solar Cells. *Materials* 8:5715-5729.
75. Sim K, Sung SJ, Jo HJ, Jeon DH, Kim DH, Kang JK (2013) Electrochemical Investigation of High-Performance Dye Sensitized Solar Cells Based on Molybdenum for Preparation of Counter Electrode. *Int J Electrochem Sci* 8: 8272-8281
76. Maiaugree W, Lowpa S, Towannang M, Rutphonsan P, Tlangtrakarn A et al (2015) A dye sensitized solar cell using natural counter electrode and natural dye derived from mangosteen peel waste. *Sci Rep* 5:15230.
77. Kudin KN, Ozbas B, Schniepp HC, Prud'homme RK, Aksay IA, Car R (2008) Raman Spectra of Graphite Oxide and Functionalized Graphene Sheets. *Nano Lett* 8:36-41
78. Puspitasari N, SSNA, Yudoyono G, Endarko E (2017) Effect of Mixing Dyes and Solvent in Electrolyte Toward Characterization of Dye Sensitized Solar Cell Using Natural Dyes as The Sensitizer. *1OP Conf. Series: Materials Science and Engineering* 214012022
79. Stergiopoulos T, Arabatzis IM, Katsaros G, Falaras P (2002) Binary Polyethylene Oxide/Titania Solid-State Redox Electrolyte for Highly Efficient Nanocrystalline TiO<sub>2</sub> Photoelectrochemical Cells. *Nano Lett* 2:1259-1261.
80. Bai S, Bu C, Tai Q, Liang L, Liu Y et al (2013) Effects of Bisimidazolium Molten Salts with Different Substituents of Imidazolium Cations on the Performance of Efficient Dye-Sensitized Solar Cells. *ACS Appl Mater Interfaces* 5:3356-3361.
81. Wang L, Zhang H, Wang C, Ma T (2013) Highly Stable Gel-State Dye-Sensitized Solar Cells Based on High Soluble Polyvinyl Acetate. *ACS Sustain Chem Eng* 1:205-208.
82. Sun KC, Sahito IA, Noh JW, Yeo SY, Im JN et al (2016) Highly efficient and durable dye-sensitized solar cells based on a wet-laid PET membrane electrolyte. *J Mater Chem A* 4:458-465.
83. Padinger F, Rittberger RS, Sariciftci NS (2003) Effects of Postproduction Treatment on Plastic Solar Cells. *Adv Funct Mater* 13(1):85-88.
84. Ravirajan P, Haque SA, Durrant JR, Poplavskyy D, Bradley DDC, Nelson J (2004) Hybrid nanocrystalline TiO<sub>2</sub> solar cells with a fluorene-thiophene copolymer as a sensitizer and hole conductor. *J Appl Phys* 95:1473-1480.

85. Jeon S, Jo Y, Kim KJ, Jun Y, Han CH (2011) High Performance Dye-Sensitized Solar Cells with Alkylpyridinium Iodide Salts in Electrolytes. *ACS Appl Mater Interfaces* 3(2):512-516.
86. Lee Rth, Liu JK, Ho JH, Chang JW, Liu BT, Wang HU, Jeng RJ (2011) Synthesis of a Series of Quaternized Ammonium Iodide-Containing Conjugated Copolymer Electrolytes and Their Application in Dye-sensitized Solar Cells. *Polym Int* 60:483-492.
87. Gratzel M, cells D-s s (2003) *J Photochem and Photobiol C: Photochem Rev* 4(2):145-153
88. Anandan S, Latha S, Maruthamuthu P (2002) Syntheses of mixed ligands complexes of Ru(II) with 4,4'-dicarboxy-2,2'-bipyridine and substituted pteridinedione and the use of these complexes in electrochemical photovoltaic cells. *J Photochem Photobiol A* 150:167-175.
89. Islam A, Sugihara H, Hara K, Singh LP, Katoh R et al Sensitization of nanocrystalline TiO<sub>2</sub> film by ruthenium (II) diimine dithiolate complexes (2001) *J. Photochem. Photobiol. A* 145:135-141.
90. A-Rawashdeh NAF, Albiss BA, Yousef MHI (2018) Graphene-Based Transparent Electrodes for Dye Sensitized Solar Cells. *IOP Conf. Ser.: Mater. Sci. Eng* 012019:305.
91. Ito S, Zakeeruddin SM, Humphry-Baker R, Liska P, Charvet R et al (2006) High-Efficiency Organic-Dye-Sensitized Solar Cells Controlled by Nanocrystalline-TiO<sub>2</sub> Electrode Thickness. *Adv Mater* 18:1202-1205.
92. Yu X, Ci Z, Liu T, Feng X, Wang C, Ma T, Bao M (2014) Influence of different electron acceptors in organic sensitizers on the performance of dyesensitized solar cells. *Dyes Pigments* 102:126-132.
93. Rehm JM, McLendon GL, Nagasawa Y, Yoshihara K, Moser J, Grätzel M (1996) Femtosecond Electron-Transfer Dynamics at a Sensitizing Dye-Semiconductor (TiO<sub>2</sub>) Interface. *J Phys Chem B* 100:9577-9578.
94. Liang M, Xu W, Cai F, Chen P, Peng B, Chen J, Li Z (2007) New Triphenylamine-Based Organic Dyes for Efficient Dye-Sensitized Solar Cells. *J Phys Chem C* 111:4465-4472.
95. Pastore M and De Angelis F; Aggregation of Organic Dyes on TiO<sub>2</sub> in Dye-Sensitized Solar Cells Models: An ab Initio Investigation. (2010) *ACS Nano* 4: 556-562.
96. Giribabu L, Singh VK, Kumar CV SY, Reddy VG, Reddy PY (2011) Organic Ruthenium(II) Polypyridyl Complex Based Sensitizer for Dye-Sensitized Solar Cell Applications. *Advances in optoelectronics* Article ID 2943538
97. Horiuchi T, Miura H, Uchida S (2003) Highly-efficient metal-free organic dyes for dye-sensitized solar cells. *Chemistry Communications* 243036-3037

98. Horiuchi T, Miura H, Sumioka K, Uchida S (2004) High Efficiency of DyeSensitized Solar Cells Based on Metal-Free Indoline Dyes. *J Am Chem Soc* 126:12218-12219
99. Ito S, Miura H, Uchida S, Takata M, Sumioka K, Liska P, Comte P, Péchyb P, Grätzel M (2008) High-Conversion-efficiency organic dye-sensitized solar cells with a novel indoline dye. *Chem Commun*:5194-5196
100. Wu Y, Marszalek M, Zakeeruddin SM, Zhang Q, Tian H, Grätzel M, Zhu W (2012) High-conversion-efficiency organic dye-sensitized solar cells: molecular engineering on D-A-T-A featured organic indoline dyes. *Energy Environ Sci* 5:8261-8272
101. Suzuka M, Hayashi N, Sekiguchi T, Sumioka K, Takata M, Hayo N, Ikeda H, Oyaizu K, Nishide H (2016) A Quasi-Solid State DSSC with 10.1% Efficiency through Molecular Design of the Charge-Separation and -transport. *Sci Rep* 6;28022
102. Irgashev RA, Karmatsky AA, Kim GA, Sadovnikov AA, Emets W, Grinberg VA et al (2017) Novel push-pull thieno[2,3-b]indole-based dyes for efficient dyesensitized solar
103. Choi H, Baik C, Kang SO, Ko J, Kang MS, Nazeeruddin MK, Grätzel M (2008) Highly efficient and thermally stable organic sensitizers for solvent-free dyesensitized solar cells. *Angew Chem Int Ed* 47:327-330.
104. Kim S, Lee JK, Kang SO, Ko J, Yum JH, Fantacci S, De Angelis F, Censo DD, Nazeeruddin MK, Grätzel M (2006) Molecular Engineering of Organic Sensitizers for Solar Cell Applications. *J Am Chem Soc* 128:16701-16707.
105. Liang M, Lu M, Wang QL, Chen WY, Han HY, Sun Z, Xue S (2011) Efficient Dye-sensitized Solar Cells with Iriarylamine Organic Dyes featuring Functionalized-Iruxene Unit. *J Power Sources* 196:1657-1664.
106. Hagberg DP, Marinado T, Karlsson KM, Nonomura K, Qin P, Boschloo G, Brinck 1, Hagfeldt A, Sun L (2007) Tuning the HOMO and LUMO energy levels of organic chromophores for dye sensitized solar cells. *J Org Chem* 72:9550-9556.
107. Xu M, Li R, Pootrakulchote N, Shi D, Guo J, Yi Z, Zakeeruddin SM, Grätzel M, Wang P (2008) Energy-Level and Molecular Engineering of Organic D-T-A Sensitizers in Dye-Sensitized Solar Cells. *J Phys Chem C* 112:19770-19776.
108. Liu WH, Wu IC, Lai CH, Chou PT, Li YT, Chen CL, Hsu YY, Chi Y (2008) Simple organic molecules bearing a 3,4-ethylenedioxythiophene linker for efficient dye-sensitized solar cells. *Chem Commun* 7:5152-5154.
109. Prachumrak N, Sudyoasuk T, Thangthong A, Nalaoh P, Jungsuttiwong S, Daengngern R, Namuangruk S, Pattanasattayavonga P, Promarak V (2017) Improvement of D-T-A organic dye-based dye-sensitized solar cell performance by

- simple triphenylamine donor substitutions on the n-linker of the dye. *Mater Chem* 1:1059-1072.
110. Hagberg DP, Edvinsson T, Marinado T, Boschloo G, Hagfeldt A, Sun L (2006) A novel organic chromophore for dye-sensitized nanostructured solar cells. *Chem Commun*:2245-2247
  111. Baheti A, Iyagi P, Justin Thomas KR, Hsu YC, T'suen Lin J (2009) Simple Triarylamine-Based Dyes Containing Fluorene and Biphenyl Linkers for Efficient Dye-Sensitized Solar Cells. *J Phys Chem C* 113(20):8541-8547.
  112. Lu M, Liang M, Han HY, Sun Z, Xue S (2011) Organic Dyes Incorporating Bis hexapropyltruxeneamino Moiety for Efficient Dye-Sensitized Solar Cells. *J Phys Chem C* 115:274-281.
  113. Qiu XP, Zhou HP, Zhang XF, Xu TH, Liu XL, Zhao YY, Lu R (2008) Synthesis of phenothiazine-functionalized porphyrins with high fluorescent quantum yields. *Tetrahedron Lett* 49:7446-1449.
  - Tian H, Yang X, Cong J, Chen R, Teng C, Liu J, Hao Y, Wang L, Sun L (2010) Effect of different electron donating groups on the performance of dyesensitized solar cells. *Dyes Pigments* 84:62-68.
  114. Tian H, Yang X, Cong J, Chen R, Teng C, Liu J, Hao Y, Wang L, Sun L (2010) Effect of different electron donating groups on the performance of dyesensitized solar cells. *Dyes Pigment* 84:62-68
  115. Zhu XQ, Dai Z, Yu A, Wu S, Cheng JP (2008) Driving Forces for the Mutual Conversions between Phenothiazines and Their Various Reaction Intermediates in Acetonitrile. *J Phys Chem B* 112:11694-11707.
  116. Wang CL, Chang YC, Lan CM, Lo CF, Diao EWG, Lin CY (2011) Enhanced light harvesting with T-Conjugated cyclic aromatic hydrocarbons for porphyrin-sensitized solar cells. *Energy Environ Sci* 4:1788-1795
  117. Wagner J, Pielichowski J, Hinsch A, Pielichowski K, Bogda D, Pajda M, Kurek SS, Burczyk A (2004) New carbazole-based polymers for dye solar cells with hole-conducting polymer. *Syn Metals* 146:159-165.
  118. Li J, Dierschke F, Wu J, Grimsdale AC, Müllen K (2006) Poly(2,7-carbazole) and perylene tetracarboxydimide: a promising donor/acceptor pair for polymer solar cells. *J Mater Chem* 16:96-100.
  119. Promarak V, Saengsuwan S, Jungsuttiwong S, Sudyoadsuk T, Keawin T (2007) Synthesis and characterization of N-carbazole end-capped oligofluorenes. *Tetrahedron Lett* 48:89-93.

120. Hwang SW, Chen Y (2002) Photoluminescent and Electrochemical Properties of Novel Poly(aryl ether)s with Isolated Hole-Transporting Carbazole and Electron-Transporting 1,3,4-Oxadiazole Fluorophores. *Macromolecules* 35:5438-5443
- 121.. Ning Z, Zhang Q, Wu W, Pei H, Liu B, Tian H (2008) Starburst Triarylamine Based Dyes for Efficient Dye-Sensitized Solar Cells. *J Org Chem* 73:3791-3797.
- 122.Wang ZS, Koumura N, Cui Y, Takahashi M, Sekiguchi H et al (2008) Hexylthiophene-Functionalized Carbazole Dyes for Efficient Molecular Photovoltaics: Tuning of Solar-Cell Performance by Structural Modification *Chem Mater* 20:3993-4003.
- 123.Koumura N, Wang ZS, Miyashita M, Uemura Y, Sekiguchi H, Cui Y, Mori A, Mori S, Hara K (2009) Substituted carbazole dyes for efficient molecular photovoltaics: long electron lifetime and high open circuit voltage performance. *J Mater Chem* 19:4829-4836.
- 124.Liu B, Wang R, Mi W, Lia X, Yu H (2012) Novel branched coumarin dyes for dye-sensitized solar cells: significant improvement in photovoltaic performance by simple structure modification. *J Mater Chem* 22:15379-15387.
125. Ye M WX, Wang M, Locozzia J, Zhang N, Lin C, Lin Z (2015) Recent advances in dye-sensitized solar cells: from photoanodes, sensitizers and electrolytes to counter electrodes. *Mater Today* 18(3):155-162.
- 126.. Cherepy NJ, Smestad GP, Grätzel M, Zhang JZ (1997) Ultrafast Electron Injection: Implications for a Photoelectrochemical Cell Utilizing an Anthocyanin Dye-Sensitized TiO<sub>2</sub> Nanocrystalline Electrode. *J Phys Chem B* 101:9342-9351.
127. Hao S, Wu J, Huang Y, Lin J (2006) Natural Dyes as Photosensitizers for Dye-Sensitized Solar Cell. *Sol Energy* 80:209-214.
128. Sutthanut K, Sripanidkulchai B, Yenjai C, Jay M (2007) Simultaneous identification and quantitation of 11 flavonoid constituents in *Kaempferia parviflora* by gas chromatography. *J Chromatogr A* 1143:227-233.
129. Kishimoto S, Maoka T, Sumitomo K, Ohmiya A (2005) Analysis of Carotenoid Composition in Petals of *Calendula* (*Calendula officinalis* L) *Biosci Biotechnol Biochem* 69:2122-2128.
- 130.Ahliha AH, Nurosyid F, Supriyanto A, Kusumaningsih T (2018) Optical properties of anthocyanin dyes on TiO<sub>2</sub> as photosensitizers for application of dye-sensitized solar cell (DSSC). *IOP Conf Series: Materials Science and Engineering* 012018:333.
- 131.. Narayan MR (2012) Review: Dye sensitized solar cells based on natural photosensitizers. *Renew Sust Energ Rev* 16:208-215.
132. Narayan M, Raturi A (2011) Investigation of some common Fijian flower dyes as photosensitizers for dye sensitized solar cells abstract. *Appl Sol energy* 47:112.

133. Ludine NA, A-AlWani Mahmoud AM, Mohamad AB, Kadhum AAH, Sopian K, Karim NSA (2014) Review on the development of natural dye photosensitizer for dye-sensitized solar cells. *Renew Sust Energ Rev* 31:386-96.
134. Suryana R (2013) Khoiruddin, Supriyanto A; Beta-Carotene Dye of *Daucus carota* as Sensitizer on Dye-Sensitized Solar Cell. *Mater Sci Forum* 737:15-19.
135. Ruiz-Anchondo T, Glossman-Mitnik D (2009) Computational Characterization of the  $\beta$ -Carotene Molecule. *J Mol Struct THEOCHEM* 913:215-220.
136. Argazzi R, Larramona G, Contado C, Bignozi CA (2004) Preparation and Photoelectrochemical Characterization of a Red Sensitive Osmium Complex Containing 444-Irizarboxy-2,2:6,2-terpyridine and Cyanide Ligands. *J Photochem Photobiol A* 164:15-21.
137. Geary EAM, Yellowlees L, Jack LA, Oswald IDH, Parsons S, Hirata N, Durrant J, Odertson N (2005) Synthesis, Structure, and properties of  $Pt(ODdiimine)(dithiolate)$  dyes with 3,3', 4,4', and 5,5'-disubstituted bipyridyl: applications in dye-sensitized solar cells. *Inorg Chem* 44:242-250.
138. Ferrere S (2002) New photosensitizers based upon  $[Fe^{II}OACN]GJ$  and  $[Fe^{II}L]L$ , where L is substituted 2,2'-bipyridine. *Inorg Chim Acta* 329:79-92
139. Margulis GY, Lim B, Hardin BE, Unger EL, Yum JH, Feckl JM, Fattakhova-Rohifing D, Bein I et al (2013) Highly soluble energy relay dyes for dye-sensitized solar cells. *Phys Chem Chem Phys* 15:11306-11312.
140. Forster T (1959) 10th Spiers Memorial Lecture. Transfer mechanisms of electronic excitation. *Discuss Faraday Soc* 2/:7-17.
141. Siegers C, Hoh-Ebinger J, Zimmermann B, Wurfel U, Mulhaupt R, Hinsch A, Haag R (2007) A Dyadic Sensitizer for Dye Solar Cells with High Energy Transfer Efficiency in the Device. *ChemPhysChem* 8:1548-1556.
142. Lin Y-J, Chen JW, Hsiao PT, Tung YL, Chang CC, Chen CM (2017) Efficiency improvement of dye-sensitized solar cells by in situ fluorescence resonance energy transfer. *J Mater Chem A* 5:9081-9089.
143. Pratiwi DD, Nurosyid F, Supriyanto A, Suryana R (2017) Efficiency enhancement of dye-sensitized solar cells (DSSC) by addition of synthetic dye into natural dye (anthocyanin). *OP Conf Series: Materials Science and Engineering* Article ID 012012:176.
144. Chang H, Kao MU, Chen TL, Chen CH, Cho KC, Lai XR (2013) Characterization of Natural Dye Extracted from Wormwood and Purple Cabbage for Dye-Sensitized Solar Cells. *J Photoenergy* Article ID 1595028.

145. Lim A, Manaf NH, Tennakoon K, Chandrakanthi RLN, Lim LBL, Sarath Bandara JMR, Ekanayake P (2015) Higher Performance of DSSC with Dyes from *Cladophora* sp. as Mixed Cosensitizer through Synergistic Effect. *J Biophys Article* ID 5104678.
146. Zhang L, Konno A (2018) Development of Flexible Dye-sensitized Solar Cell Based on Predeposited Zinc Oxide Nanoparticle. *Int J Electrochem Sci* 13344-352
147. Gangishetty MK, Lee KE, Scott RWJ, Kelly TL (2013) Plasmonic Enhancement of Dye Sensitized Solar Cells in the Red-to-near-infrared Region using Triangular Core-Shell Ag@SiO<sub>2</sub> Nanoparticles. *ACS Appl Mater Interfaces* 5: 11044-11051.
148. Hossain MA, Park J, Yoo D, Baek YK, Kim Y, Kim SH, Lee D (2016) Surface Plasmonic Effects on Dye-Sensitized Solar Cells by SiO<sub>2</sub>-Encapsulated Ag Nanoparticles. *Curr Appl Phys* 16:397-403.
149. Ihara M, Kanno M, Inoue S (2010) Photoabsorption-Enhanced Dye Sensitized Solar Cell by Using Localized Surface Plasmon of Silver Nanoparticles Modified with Polymer. *Phys E Low Dimens Syst Nanostruct* 42:2867-2871.
150. Jun HK, Careemb MA, Arof AK (2016) Plasmonic effects of quantum size gold nanoparticles on dye-sensitized solar cell. *Materials Today: Proceedings* 35:573-579
151. Baxter JB (2012) Commercialization of dye sensitized solar cells. *J Vac Sci Technol A: Vacuum, Surfaces, and Films* 30(2):020801.
152. Desilvestro H, Bertozzi M, Tulloch S, Tulloch GE (2010) Packaging, Scale-up, and Commercialization of Dye Solar Cells. In: Kalyanasundaram K (ed) *Dye sensitized solar cells*. CRC Press, Lausanne.
153. Berginc M, Krasovec UO, Topic M (2014) Outdoor ageing of the dye sensitized solar cell under different operation regimes. *Krasovec Sol Energy Mater Sol Cells* 120:491-499